

# A next-generation Fab library platform directly yielding drug-like antibodies with high affinity, diversity, and developability

Fortunato Ferrara, Adeline Fanni, Andre A. R. Teixeira, Esteban Molina, Camila Leal-Lopes, Ashley DeAguero, Sara D'Angelo, M. Frank Erasmus, Laura Spector, Luis Antonio Rodriguez Carnero, Jianquan Li, Thomas J. Pohl, Nikolai Suslov, Klervi Desrumeaux, Conor McMahon, Sagar Kathuria & Andrew R. M. Bradbury

To cite this article: Fortunato Ferrara, Adeline Fanni, Andre A. R. Teixeira, Esteban Molina, Camila Leal-Lopes, Ashley DeAguero, Sara D'Angelo, M. Frank Erasmus, Laura Spector, Luis Antonio Rodriguez Carnero, Jianquan Li, Thomas J. Pohl, Nikolai Suslov, Klervi Desrumeaux, Conor McMahon, Sagar Kathuria & Andrew R. M. Bradbury (2024) A next-generation Fab library platform directly yielding drug-like antibodies with high affinity, diversity, and developability, *mAbs*, 16:1, 2394230, DOI: [10.1080/19420862.2024.2394230](https://doi.org/10.1080/19420862.2024.2394230)

To link to this article: <https://doi.org/10.1080/19420862.2024.2394230>



© 2024 The Author(s). Published with license by Taylor & Francis Group, LLC.



[View supplementary material](#)



Published online: 27 Aug 2024.



[Submit your article to this journal](#)



Article views: 1890



[View related articles](#)



















[View Crossmark data](#)

REPORT



## A next-generation Fab library platform directly yielding drug-like antibodies with high affinity, diversity, and developability

Fortunato Ferrara <sup>a\*</sup>, Adeline Fanni <sup>a\*</sup>, Andre A. R. Teixeira <sup>b†</sup>, Esteban Molina <sup>a</sup>, Camila Leal-Lopes <sup>b‡</sup>, Ashley DeAguero <sup>a</sup>, Sara D'Angelo <sup>a</sup>, M. Frank Erasmus <sup>a</sup>, Laura Spector <sup>a</sup>, Luis Antonio Rodriguez Carnero <sup>b</sup>, Jianquan Li <sup>a</sup>, Thomas J. Pohl <sup>a</sup>, Nikolai Suslov <sup>c§</sup>, Klervi Desrumeaux<sup>d</sup>, Conor McMahon <sup>c</sup>, Sagar Kathuria <sup>c</sup>, and Andrew R. M. Bradbury <sup>a</sup>

<sup>a</sup>Specifica LLC, a Q<sup>2</sup> Solutions Company, Santa Fe, NM, USA; <sup>b</sup>New Mexico Consortium, Los Alamos, NM, USA; <sup>c</sup>Sanofi, Large Molecule Research, Cambridge, MA, USA; <sup>d</sup>Sanofi, Large Molecule Research, Vitry-sur-Seine, France

### ABSTRACT

We previously described an *in vitro* single-chain fragment (scFv) library platform originally designed to generate antibodies with excellent developability properties. The platform design was based on the use of clinical antibodies as scaffolds into which replicated natural complementarity-determining regions purged of sequence liabilities were inserted, and the use of phage and yeast display to carry out antibody selection. In addition to being developable, antibodies generated using our platform were extremely diverse, with most campaigns yielding sub-nanomolar binders. Here, we describe a platform advancement that incorporates Fab phage display followed by single-chain antibody-binding fragment Fab (scFab) yeast display. The scFab single-gene format provides balanced expression of light and heavy chains, with enhanced conversion to IgG, thereby combining the advantages of scFvs and Fabs. A meticulously engineered, quality-controlled Fab phage library was created using design principles similar to those used to create the scFv library. A diverse panel of binding scFabs, with high conversion efficiency to IgG, was isolated against two targets. This study highlights the compatibility of phage and yeast display with a Fab semi-synthetic library design, offering an efficient approach to generate drug-like antibodies directly, facilitating their conversion to potential therapeutic candidates.

### ARTICLE HISTORY

Received 20 June 2024  
Revised 13 August 2024  
Accepted 15 August 2024

### KEYWORDS




Recombinant antibody libraries; Fab; phage display; yeast display; developability

## Introduction

Over 130 therapeutic antibodies have been approved in the US ([www.antibodysociety.org/antibody-therapeutics-product-data](http://www.antibodysociety.org/antibody-therapeutics-product-data)), with immunization being the commonest method used to generate leads, notwithstanding notable drawbacks, such as difficulties in obtaining antibodies with highly specific or challenging recognition specificities,<sup>1</sup> the need to clone V genes for downstream engineering (including humanization for wild-type mice), developability improvement, the time needed for the immune response, the use of animals, and, thus, the lack of suitability for non-immunogenic or highly toxic targets. Display technologies, on the other hand, can easily provide antibodies against non-immunogenic or highly toxic targets, and careful selection procedures can direct binding to specific epitopes, conformations, isoforms, or cross-reactivities. Phage and yeast display<sup>1</sup> are the most successful antibody discovery display platforms, and particularly powerful when combined.<sup>2–4</sup> Phage libraries provide enormous initial diversity, while the

ability to use fluorescent-activated cell sorting (FACS) with yeast libraries affords tremendous versatility, allowing fine-tuning of specific binding properties after diversity has been reduced to a broadly binding population by a couple of rounds of phage display. Notwithstanding the dominance of immunization, display technologies are widely used in the discovery of diagnostic and therapeutic antibodies and may replace immunization as the preferred way to generate therapeutic antibodies given the enormous recent improvements in libraries and selection methods.<sup>4–9</sup>

The single-chain variable fragment (scFv) format<sup>10</sup> has been the format of choice for many groups,<sup>6,11–16</sup> with the antigen-binding fragment (Fab) format an alternative.<sup>17–24</sup> Both have their advantages and disadvantages. For example, scFvs are generally less stable, more prone to aggregation and more challenging to convert to full-length IgG,<sup>25–28</sup> while Fabs are larger molecules requiring two separate polypeptide chains to be precisely assembled with a disulfide bond, resulting in worse folding, decreased solubility, display and lower expression level in


**CONTACT** Fortunato Ferrara  [fortunato.ferrara@q2labsolutions.com](mailto:fortunato.ferrara@q2labsolutions.com); Andrew R. M. Bradbury  [andrew.bradbury@q2labsolutions.com](mailto:andrew.bradbury@q2labsolutions.com)  Specifica LLC, a Q<sup>2</sup> Solutions Company, 1607 Alcala Street, Suite 202, Santa Fe 87501, NM, USA

\*Equal contribution.

†Present address: Institute for Protein Innovation, Boston, MA, USA

‡Present address: Sanofi, Large Molecule Research, Cambridge, MA, USA

§Present address: Phenomic Bio Inc, Waltham, MA, USA

 Supplemental data for this article can be accessed online at <https://doi.org/10.1080/19420862.2024.2394230>.

© 2024 The Author(s). Published with license by Taylor & Francis Group, LLC.

This is an Open Access article distributed under the terms of the Creative Commons Attribution-NonCommercial License (<http://creativecommons.org/licenses/by-nc/4.0/>), which permits unrestricted non-commercial use, distribution, and reproduction in any medium, provided the original work is properly cited. The terms on which this article has been published allow the posting of the Accepted Manuscript in a repository by the author(s) or with their consent.

*Escherichia coli* (*E. coli*).<sup>29</sup> While over 100 phage-based antibody libraries have been described (see<sup>9</sup> for an overview), very few scFv<sup>30</sup> or Fab<sup>27,31,32</sup> libraries have been displayed on yeast, with yeast mating, rather than cloning, being the commonest way to generate diversity in Fab libraries. The need to separately express VH and VL chains can result in the display of unpaired VH-CH1 chains with specific binding activity in both yeast<sup>27</sup> and phage display formats,<sup>33,34</sup> the selection of which can result in the domination of selection outputs by heavy-chain only binding clones, rather than desired binders containing both VH and VL chains, a problem that can be mitigated by staining yeast with reagents specific for the soluble chain, rather than that tethered to the yeast surface.

A single-chain Fab (scFab) format, inspired by a previously described single-chain IgG format,<sup>35</sup> has also been developed,<sup>36</sup> in which a linker connects the C terminus of the CL with the N terminus of the VH (or *vice versa*), and has been used in phage,<sup>36–39</sup> yeast<sup>39–41</sup> and mammalian display.<sup>42</sup> In theory, the scFab format should combine the main advantages of scFv and Fab, in that it is encoded by a single gene format, but also comprises both CH1 and CL, which are expected to impart additional stability and more straightforward conversion to IgG. However, like scFvs,<sup>5,6</sup> not all IgGs convert effectively into scFabs<sup>40</sup> and not all scFabs convert into IgGs,<sup>43</sup> and there is some uncertainty as to whether the scFab format displays better than the traditional Fab.<sup>40</sup> Here, we explore the display of scFabs and their conversion into IgG.

In this study, we describe a Fab phage display library built using the same principles previously developed for a scFv library<sup>6</sup> that generated extremely high affinity antibodies.<sup>4,5,44</sup> A key feature of that platform was the combination of phage and yeast display: phage display was used to reduce diversity to an enriched binding population, while yeast display was then used to sort for high affinity binders by FACS. While transfer from Fab-phage display to Fab-yeast display is feasible, we reasoned that transferring Fab-phage to scFab-yeast avoided the limitations of Fab display on yeast, ensuring balanced expression and display of VH and VL chains, whereas in the traditional Fab format, either VH or VL may be overexpressed relative to the other, resulting in chain imbalance.

## Materials and methods

### Library construction

Construction of the Fab phage display library was performed following the general strategy described in Teixeira et al.<sup>6</sup> where an scFv library was developed and validated. Briefly, the Fab library is a semi-synthetic library, where the natural HCDR3 diversity is recovered from CD19<sup>+</sup> B-cells obtained from fresh leukapheresis of 10 healthy human donors, while the germline

matched LCDR1–3 and HCDR1–2 diversity were obtained from a NGS dataset derived from 40 donors, where all sequence liabilities and anomalous lengths were excluded, as previously described.<sup>6</sup> Oligonucleotides encoding HCDR1–2 and LCDR1–3, from which the sequence liabilities were purged, were synthesized on an array-based platform (Agilent). The different CDR collections (e.g., HCDR1, HCDR2) were individually cloned into five different scFv scaffolds corresponding to the Fabs (Table 1) and filtered for well-expressing CDRs by yeast display, as previously described.<sup>6</sup> We have found that cloning the different oligo-synthesized CDR collections into an scFv format as single CDR libraries, and sorting/filtering for well-displaying CDRs helps improve the quality of the library. The filtered CDRs are then recovered and cloned into the final Fab scaffolds, as shown in Figure 2a. The filtered CDRs from each of the libraries were subsequently amplified along with their flanking framework regions. VL-CL and VH-CH1 were first assembled separately and finally combined into a VL-CL – VH-CH1 PCR product. The Fab amplicons were digested using BssHII and NheI (R0131L and R0199L, NEB) and ligated into the pANDA5 Fab phagemid vector, derived from the pDAN5 scFv vector<sup>15</sup> previously digested with the same enzymes. pANDA5 differed from pDAN5 by having: 1) no lox site between heavy and light chains; 2) having the VL coupled to a codon-optimized light chain constant region and the VH with a IgG1 derived, codon-optimized, CH1; 3) using a truncated form of g3p in place of the full length, and 4) having two independent PelB-derived leaders for the expression of the two antibody domains. Ligation products were transformed into *E. coli* TG1 strain (60502–2, Lucigen) by electroporation to obtain  $\sim 1.6 \times 10^{10}$  transformants.

### Sanger analysis of Fab library and ELISA assessment of display in the naïve library packaging

A total of 192 clones obtained from directly plating serial dilutions of each Fab sub-library (prepackaging) were sequenced using primers upstream and downstream of the region encoding the Fab sequences. Sequence data were filtered for an average Q-score  $\geq 40$ , no mixed traces, no ambiguity at VL or VH and non-redundant (clone picked twice by accident). Valid clones containing open reading frames were classified as functional.

For post-packaging analysis, polyclonal phage was generated from the naïve library and used to infect *E. coli* cells, followed by single colony picking and sequencing as described above.

The same colonies used for Sanger Sequencing, pre- and post-packaging, were used to produce monoclonal phage, and tested in a sandwich ELISA. 96-well microtiter plates were coated with anti-Fab antibody (I5260, Millipore Sigma) in phosphate-buffered saline (PBS) overnight at 4°C, blocked with 5% milk, incubated with supernatant from phage cultures

**Table 1.** Scaffolds used to build the Fab phage display library.

Library	Therapeutic	Clinical status	Type	VH germline	VL germline	Original target	Heavy fr1-3 mutations from germline	Light fr1-3 mutations from germline
Lib1A	Abrilumab (1A)	Phase 2	Human	VH1-24	Vk1-12	$\alpha 4\beta 7$ integrin	2	1
Lib3B	Crenezumab (3B)	Phase 3*	Humanized	VH3-7	Vk2-28	1-40 $\beta$ -amyloid	3	1
Lib4A	Necitumumab (4A)	Approved	Human	VH4-30-4	Vk3-11	EGFR	4	1
Lib7A	-	-	Human	VH3-48	Vk1-33	-	3	0
Lib8B	Adalimumab (8B)	Approved	Human	VH3-9	Vk1-27	TNFA	4	1

for 1 h, washed, and probed with anti-M13 antibody coupled with horseradish peroxidase (HRP) (11973-MM05T-H, Sino Biological). Wells showing signal 5-fold above background were considered positive for display.

### **Pacbio sequencing and analysis**

The entire Fab cassette was amplified from the cloned library using specific flanking primers, gel purified, and sequenced using Pacbio Sequel II. Reads were filtered for length (1,000 to 1,300 bp), quality (all bases with Q-score  $\geq 75$ ) and annotated using an internal tool (IgMatcher, available from [eyesopen.com/orion/antibody-discovery-suite](https://eyesopen.com/orion/antibody-discovery-suite)). For the calculation of frequency, clones were defined by the concatenated CDR sequences.

### **Novaseq sequencing**

The VH portion of the cloned library was amplified using flanking specific primers, gel purified, and sequenced in a single lane of Novaseq S4  $2 \times 150$ bp. The HCDR3 sequences were extracted, translated and only functional sequences (in frame and no stop codons) were considered for diversity calculations.

### **Fab library phage production and QC**

Phage particles were produced by inoculating bacteria from each of the five libraries into terrific broth (TB) media + 3% dextrose + 100  $\mu$ g/ml carbenicillin and growing at 37°C to  $OD_{600nm} = 0.5$ . The bacteria were then infected with the helper phage M13K07 (MOI = 10) and grown overnight in TB media + 100  $\mu$ g/ml carbenicillin and 50  $\mu$ g/ml kanamycin at 25°C for phage production. The following day, phages were precipitated from the supernatant using PEG/NaCl. Western blot analysis of Fab displayed on phage particles was performed on PEG precipitated phage from each sub-library by electrophoresis using the NuPAGE gel system (Life Technologies). After electrophoresis, proteins were transferred to nitrocellulose using a semidry blot apparatus. The membrane was blocked with 3% milk PBST for 1 h at room temperature. This was then incubated in 1 mg/ml of anti-Myc-HRP conjugated antibody (ThermoFisher, Cat# MA1-21316-HRP, RRID:AB\_2536997) in 2% milk PBST for 1 h at room temperature. The blot was washed  $2 \times$  PBST and  $1 \times$  PBS for 5 min each. After washing, the HRP activity was detected using chemiluminescent substrates (ThermoFisher, Cat# 34075).

### **Fab phage-display selection**

Fab fragments were selected by phage display from the library using a previously described protocol.<sup>2,3</sup> Briefly, selections were carried out in parallel in solution on two target antigens using phage produced from each of the five separate sub-libraries. The selections were performed using the automated Kingfisher magnetic bead system (ThermoFisher) using 320 nM of biotinylated hIFN $\alpha$ -2b (GenScript, Cat # Z03002) or 330 nM of biotinylated SARS-CoV-2 RBD (ACRO Biosystems, Cat # SPD-C82E9). Targets were incubated with the phage

antibody library, and binding phage captured using streptavidin conjugated magnetic beads (Dynabeads M-280, ThermoFisher, Cat # 11205D). Non-binding phage was removed with a series of washing steps. After propagation of the eluted phages, the selection cycle was repeated for a total of three rounds. Increased stringency (longer washes) was used in the second and third selection rounds. Bound phages are recovered from the beads by acid elution and used to infect XL1Blue (Agilent). Ninety-five bacterial colonies from the final selected populations were Sanger sequenced to assess diversity of the antibody population and screened by phage ELISA in parallel (see below). Clone sequences were included in the analysis if they fulfilled the following criteria: both forward and reverse reads have an average Q-score  $\geq 40$ ; both forward and reverse reads are free of mixed traces in the CDR regions; no ambiguous nucleotides in either VL or VH; functional clones were defined as lacking frameshifts or stop-codons in VL or VH regions, having the correct JK/CK junction (last 3 bp in JK and first 30 bp in CK checked), and having the correct signal sequence upstream of VH (30 last bp of the signal sequence checked).

### **Phage ELISA**

Phage ELISA was performed to determine binding activity of the polyclonal phage after three rounds of selection and for monoclonal binding validation before Sanger sequencing screening. ELISA wells (Nunc Maxisorp) were coated with 0.5  $\mu$ g neutravidin per well overnight at 4°C. The following day, after washing away the excess neutravidin, 0.2  $\mu$ g per well of biotinylated hIFN $\alpha$ -2b or SARS-CoV-2 RBD or a 1:700 dilution of anti-Human IgG Fab-specific antibody in PBS (Millipore Sigma-Aldrich, Cat #I5260-1 mL, RRID:AB\_260206) were added. Polyclonal phages were diluted 1:10 in PBS containing 5% (w/v) skim milk. Monoclonal phage supernatant was diluted 1:1 in phosphate-buffered saline (PBS) containing 5% (w/v) skim milk. Diluted phages were incubated in the antigen-coated wells for 1 h at room temperature. After a rinse step, anti-M13- horseradish peroxidase (HRP) (SinoBiological, Cat# 11973-MM05T-H), was added and incubated for 1 h at room temperature to detect the binding phage. 3,3',5,5'-tetramethylbenzidine (TMB) was used to develop the colorimetric assay, which was stopped with 1 M H<sub>2</sub>SO<sub>4</sub>. The signal was measured at absorbance 450 nm.

### **Two-step PCR conversion of Fab phage display into scFab yeast display**

The overall strategy is illustrated in Figure 2. After isolating the Fab phage display vector by miniprepping, an inverse PCR was performed with primers design to overlap with the linker (primers are described in Supplementary Table S1B). The inverse PCR product was then treated with DpnI (New England Biolabs, Cat # R0176S) to digest the methylated (parental) vector and was gel purified. In parallel, the linker was PCR amplified, cleaned (Zymo Research, Cat # D4004), and cloned into the product of the inverse PCR by homologous recombination using the NEBuilder<sup>®</sup> HiFi DNA Assembly Master Mix (New England Biolabs, Cat # E2621L), to generate

scFabs within the phage vector. These scFabs were PCR amplified with primers containing 5' overhangs that overlapped with the yeast vector and were cloned into the yeast vector by gap-repair (EBY100).<sup>45</sup>

### **scFab yeast display selection**

The yeast transformed with the scFab yeast display vector were induced to display scFab and enriched for specific binders by flow cytometry-guided sorting (FACSARIA, Becton Dickinson), using previously described protocols.<sup>2,3</sup> The final binding populations were further characterized at the monoclonal level by miniprepping the final yeast output and transforming One Shot™ OmniMAX™ 2 T1R Chemically Competent *E. coli* (Thermo Fisher, Cat # C854003). Ninety-five isolated colonies were Sanger sequenced (Supplementary Table S2 for primer sequences) to identify unique clones that were then transformed back into yeast to evaluate the binding of the scFab to their target. A unique clone was defined as a binder if the binding fluorescence was 5-fold higher than the background fluorescence generated in the presence of an off-target.

### **Generation of amplicons for PacBio sequencing for selection outputs**

The yeast previously transformed with the scFab yeast display vector were diluted to OD<sub>600</sub> = 0.5 in 10 mL of yeast selective media (SD-CAA), supplemented with kanamycin and tetracycline, and grown at 30°C overnight at 250 rpm to reach OD<sub>600</sub> ≥ 4. Four mL of culture was pelleted and vortexed with an equal volume of 0.5 mm glass beads (BioSpec Products, Cat # 11079105) in Qiagen buffer P1 and subjected to vigorous vortexing for 10 min, before proceeding with the Qiagen QIAprep Spin Miniprep Kit protocol. Extracted DNA was stored on ice and used the same day. The Fab portion of the cloned sublibraries was PCR amplified using high fidelity polymerase (NEB, Cat # M04916S) and the primers VL-NGS-F and JH-NGS-R (Supplementary Table S2) with a unique combination of forward and reverse in-line barcodes for each sample. A 5 µl of each sample were run on a 1% agarose gel and BioRad Image Lab software was used to perform relative quantification of the appropriate ~1300 bp band. Samples were pooled equally by mass, and pooled PCR products were gel purified. Purified samples were eluted and quantified using a Qubit fluorometer and 500 ng of the PCR amplicons were used to prepare a library for sequencing on a PacBio Sequel II using a 15-h run (service provided by BYU-DNA sequencing center).

### **PacBio data processing and analysis**

The CCS FASTQ reads were first filtered for length and per-base quality: reads are retained if they are 1000–1300 bp and every base call has a quality score of ≥Q40. Reads were then annotated using AbXtract, Specifica's annotation tool against the scaffolds used to construct the library. The presence of specific sequence liabilities was tabulated across each of the six CDRs independently. Sequences having the same HCDR3 length and ≥90% identity in the HCDR3 amino acid sequences were defined as being in the same cluster. Functional reads

were those defined as having VL-CL and VH-CH1 in-frame and without premature stop codons or truncation. Bioinformatic analyses were performed using AbXtract ([www.eyesopen.com/orion/antibody-discovery-suite](http://www.eyesopen.com/orion/antibody-discovery-suite)).

### **Assembly of the variable scFab domains into linear expression cassettes and expression of recombinant antibodies**

A PCR-based strategy based on the methods described in Zhang et al.<sup>46</sup> was used to recover paired light and heavy chains from selected scFabs, generating transcription and translation compatible linear DNA expression cassettes (LEC) encoding whole IgG molecules. The purified LEC were transfected into Expi293F cells (Thermo Fisher Scientific), expressed, harvested, and immediately used for assessment of antibody quantification and binding to antigen as previously described.<sup>46</sup>

### **IgG validation: binding (ELISA assay)**

ELISA assays were performed to determine the binding activity of the IgG as molecules present in the supernatant of cell cultures or after purification. ELISA wells (Nunc Maxisorb) were coated directly overnight at 4°C with 0.2 µg per well of hIFNα-2b or SARS-CoV-2 RBD (non-biotinylated) or indirectly with 0.5 µg neutravidin per well overnight at 4°C, and the following day, after washing away excess neutravidin, 0.2 µg per well of biotinylated hIFNα-2b or SARS-CoV-2 RBD was added. Cell culture supernatant was diluted 1:1 in PBS, while purified IgGs was used at 0.5 µg/mL, also diluted in PBS. Diluted cell culture supernatant or IgGs were incubated in the antigen-coated wells for 1 h at room temperature. After a rinse step, anti-human-Fc-HRP (Jackson ImmunoResearch, Cat # 109-035-008, RRID:AB\_2337579) was added and incubated for 1 h at room temperature to detect binding antibodies. After a final rinse step, TMB was used to develop the colorimetric assay, which was stopped with 1 M H<sub>2</sub>SO<sub>4</sub>. The signal was measured at absorbance 450 nm.

### **IgG validation: affinity determination and developability assessment**

Kinetic assessment was performed by single cycle kinetics on an LSA Carterra. We activated a 2D planar carboxymethyl dextran (CMDP), <5 nm coating thickness chip (Carterra Cat #4282) with 33 mM of N-hydroxysulfosuccinimide (Sigma Cat #56485), 133 mM N-(3-dimethylaminopropyl)-N'-ethylcarbodiimide hydrochloride (Sigma Cat #E7750) diluted in 0.1 M MES, pH 5.5 for 5 min. An anti-human Fc (Southern Biotech, Cat #2048-01) was diluted to 50 µg/mL in 10 mM acetate, pH 4.33, and immobilized on the chip for 7.5 min. The chip surface was deactivated with 1 M ethanolamine, pH 8.5, to prevent additional primary amine coupling. For high ligand density settings, in separate experiments, anti-hIFNα-2b antibodies and anti-RBD were diluted to 10 µg/mL in 1×HBSTE (Carterra Cat #3630) and printed onto the chip for 15 min. Antigen was prepared across a 7-point dilution series from 300 nM to 412 pM. For low ligand density, antibodies were diluted to 0.5 µg/mL in

1×HBSTE and printed onto chip for 15 min. Antigens were injected across a 6-point series from 100 nM to 412 pM diluted in 1×HBSTE supplanted with 0.5 mg/mL bovine serum albumin. Each antigen dilution series measurement was carried out using non-regenerative conditions. Association was set to 5 min, dissociation to 10 min per cycle. Binding kinetics were fit using a 1:1 binding model using the Kinetics software suite (Carterra).

### **IgG developability**

Antibodies, in the IgG format, were assessed for developability using different methods to provide insight into hydrophobicity, tendency for self-association, stability, aggregation, and electrostatics. HIC was carried out using methods described previously.<sup>47</sup> Briefly, 5 µg of IgG at 1 mg/mL (spiked with a solution of 1.5 M ammonium sulfate and 0.025 M sodium phosphate at pH 7.0 corresponding to mobile phase A) were injected into a MAbPac HIC-10, 5 µm, 4.6 × 250 mm column. A linear gradient of mobile phase A and mobile phase B (0.025 M sodium phosphate, pH 7.0) was flowed through the column at 1 mL/min for 30 min while absorbance was collected at 280 nm. The main peak was collected by assessment of the chromatograph as captured as the area under the curve (AUC) of this peak relative to other peaks across the profile. Size-exclusion chromatography (SEC) was carried out using isocratic conditions and a running buffer of 10 mM sodium phosphate, 1.8 mM potassium phosphate, 137 mM sodium chloride, 2.7 mM potassium chloride at pH 7.4 (PBS) with absorbance collected at 280 nm. Samples were diluted to 1 mg/mL and 10 µL injected into a size-exclusion column (Superdex 200 Increase 5/150 GL Cat # 28-9909-45) using a Waters uHPLC. The percentage of the main peak was calculated by looking at the AUC of the main peak relative to higher molecular weight (shorter retention times) and lower molecular weight (longer retention times) peaks. The melting temperature ( $T_m$ ) corresponding to the Fab and the aggregation onset temperature were analyzed using the UNcle system (Unchained Labs). Samples were prepped into PBS, pH 7.4 and adjusted to 1 mg/mL. Aliquots of the mAb at 8.9 µL were pipetted onto the 16-well UNcle quartz capillary slides ensuring no bubbles were introduced. A temperature ramp was programmed using the software starting at 25°C and increasing to 95°C. An excitation laser at 266 nm was used and intrinsic fluorescence detected between 300 nm and 700 nm. We used the barycentric mean (BCM) of the fluorescence spectra to calculate the thermal unfolding curve, and  $T_m$  was determined from the inflection point of the BCM curve. The aggregation onset temperature ( $T_{onset}$ ) was assessed from the static light scattering (SLS) data by plotting light scattering intensity as a function of the temperature and identified as that temperature at which a significant elevation of light scattering is first observed. cGE was carried out on an Labchip GX Touch. Samples were prepped by buffer exchange into PBS, pH 7.4. The purity assessment was performed using the Protein Clear HT kit. All analysis was carried out by assessing the AUC of the peaks to determine the relative abundance of each species across the profile, with percent purity captured by dividing the AUC of the target peak by the total AUC of all peaks across the electropherogram. UV absorbance spectroscopy and DLS was carried

out using the Stunner instrument. Samples were prepared in PBS, pH 7.4 and adjusted to 0.5 mg/mL. The UV-Vis spectrum from 220 nm to 700 nm was measured. For the DLS analysis, the scattered light intensity fluctuations were recorded and an autocorrelation function calculated whereby the size distribution of the mAb samples including the Peak Interest Mean Diameter (nm) was obtained. The Peak of Interest Mass (%) was calculated as relative mass percent of the monomeric antibody species relative to other species. The Polydispersity Index (PDI) was obtained using the size distribution width.

## **Results**

### **Validation of the therapeutic scaffolds as Fab displayed on phage and as scFab displayed on yeast**

The Fab phage display library was constructed using the previously described Generation 3 concept.<sup>6</sup> Four therapeutic antibody scaffolds were used: abrilumab (VH1-24, Vk1-12), crenezumab (VH3-7, Vk2-28), necitumumab (VH4-30-4, Vk3-11), adalimumab (VH3-9, Vk1-27) and a fifth non-therapeutic scaffold (VH3-48, VK1-33) (Table 1), all chosen for their excellent developability properties.<sup>48</sup>

The five different therapeutic antibodies used as scaffolds were first expressed and displayed as Fab on phage (Figure 1a) and characterized in terms of a) infectivity by titration; b) display by Western blot; c) functionality by binding to the specific antigen (when available as a recombinant protein) and d) display level by ELISA. All five phage displaying therapeutic antibodies showed similar infectivity in the  $10^{12}$  cfu/mL range (Figure 1b). The phages successfully displayed the Fab molecule as shown by the Western blot anti-Myc (Figure 1c) and their functional display and specific binding to the targets (Figure 1d).

The Fab-phage display vectors containing the therapeutic scaffold were minipreped and converted into scFab intended for yeast display, as described in Figure 2c–g, and their functionality was tested by flow cytometry by checking their display level and the specific target binding (Figure 1e). All five scaffolds showed scFab display (>70% SV5-PE signal) and minor to no binding to the off-target. Furthermore, scFab 1A, 4A and 8B bind their specific antigens (targets for scFabs 3B and 7A were not available). A similar cloning strategy was applied to convert the five scaffolds from Fab displayed on phage into Fab displayed on yeast to compare the performance of Fab and scFab in the yeast display format. This showed incremental improvement of the expression and target binding for scFabs compared to Fab (Supplementary Figure S1).

### **Library design, construction, and quality control**

Akin to the previously described scFv libraries,<sup>6</sup> gene-family-specific human CDRs derived from next-generation sequencing (NGS) data were inserted into LCDR1–3 and HCDR1–2. This was carried out by synthesizing oligonucleotides encoding CDRs in array-based formats (Agilent), excluding those containing sequence liabilities. The final number of CDRs inserted at each position ranged from 112 (LCDR1 of Lib3B) to 74,542 (LCDR3 of Lib1A, 7A, and 8B), with the lower number of CDRs in the Lib3B LCDRs reflecting the lower

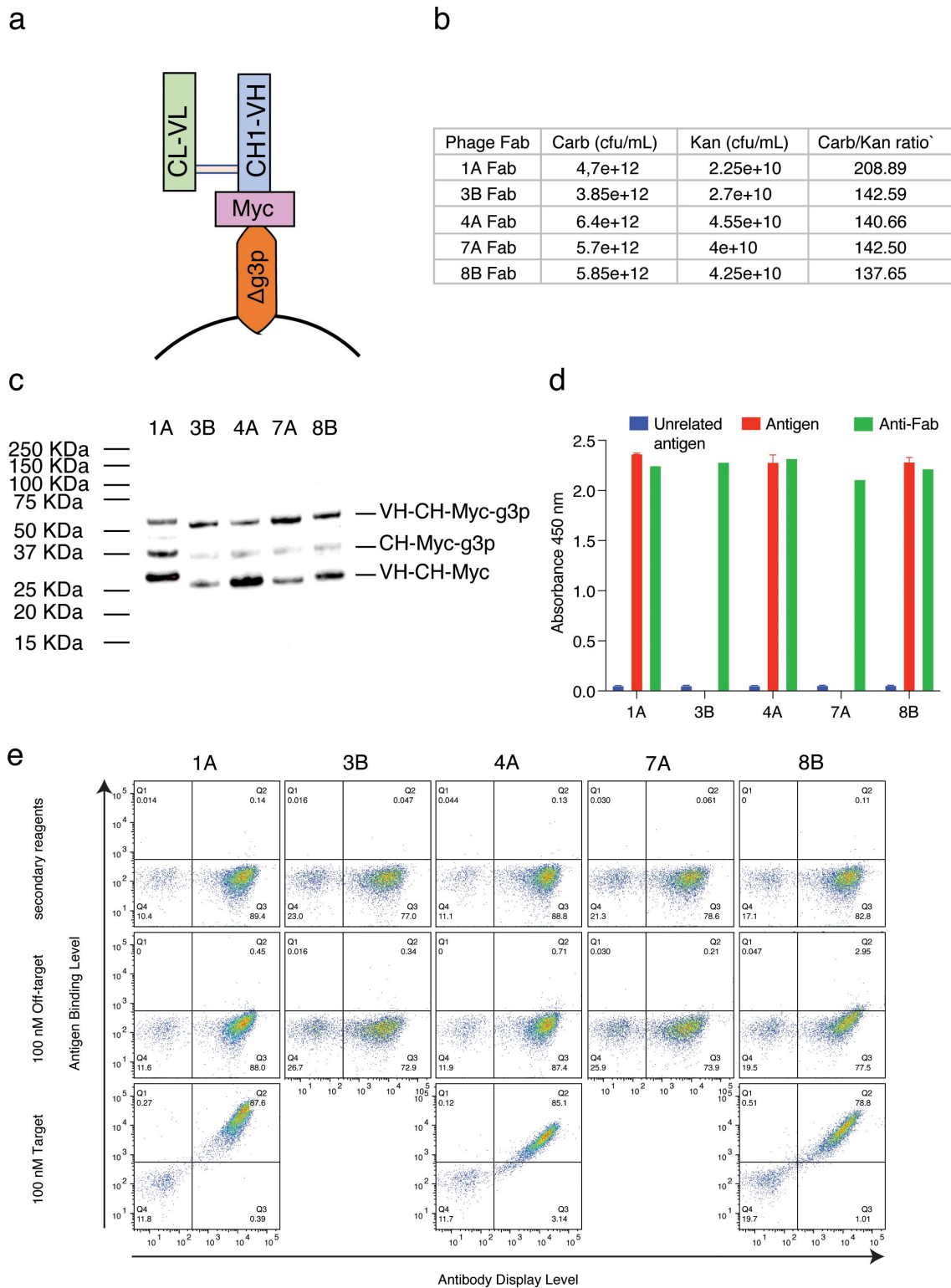


**Figure 1.** Characterization of the therapeutic Fab-phage. (a) schematic representation of library design and assembly. (b) titers of monoclonal Fab phage displaying therapeutic scaffold Fabs infection evaluated on XL1 blue cells. (c) Western blot of Fab-phage displaying therapeutic scaffolds with an anti-Myc antibody. (d) Fab phage ELISA testing the specificity of each of the therapeutic antibody scaffolds for binding to their corresponding antigens (when available as recombinant protein). An unrelated antigen was used as negative control and anti-Fab antibody was used to detect the display. (e) binding specificity of each of the therapeutic antibody scaffolds when displayed as scFab on yeast to their corresponding antigens (when available as recombinant protein). Yeast cells were tested only with the secondary reagents, as well as an unrelated antigen (off-target).

diversity of the V<sub>k</sub>2 family. To filter for functionality, CDRs were inserted into the scaffolds, a single site at a time, creating five mini-libraries for each scaffold with diversity in only one

region (5 CDR libraries per scaffold). These were displayed on yeast as scFv and filtered for expression using magnetic-assisted cells sorting.<sup>49</sup> This step ensures that only in-frame

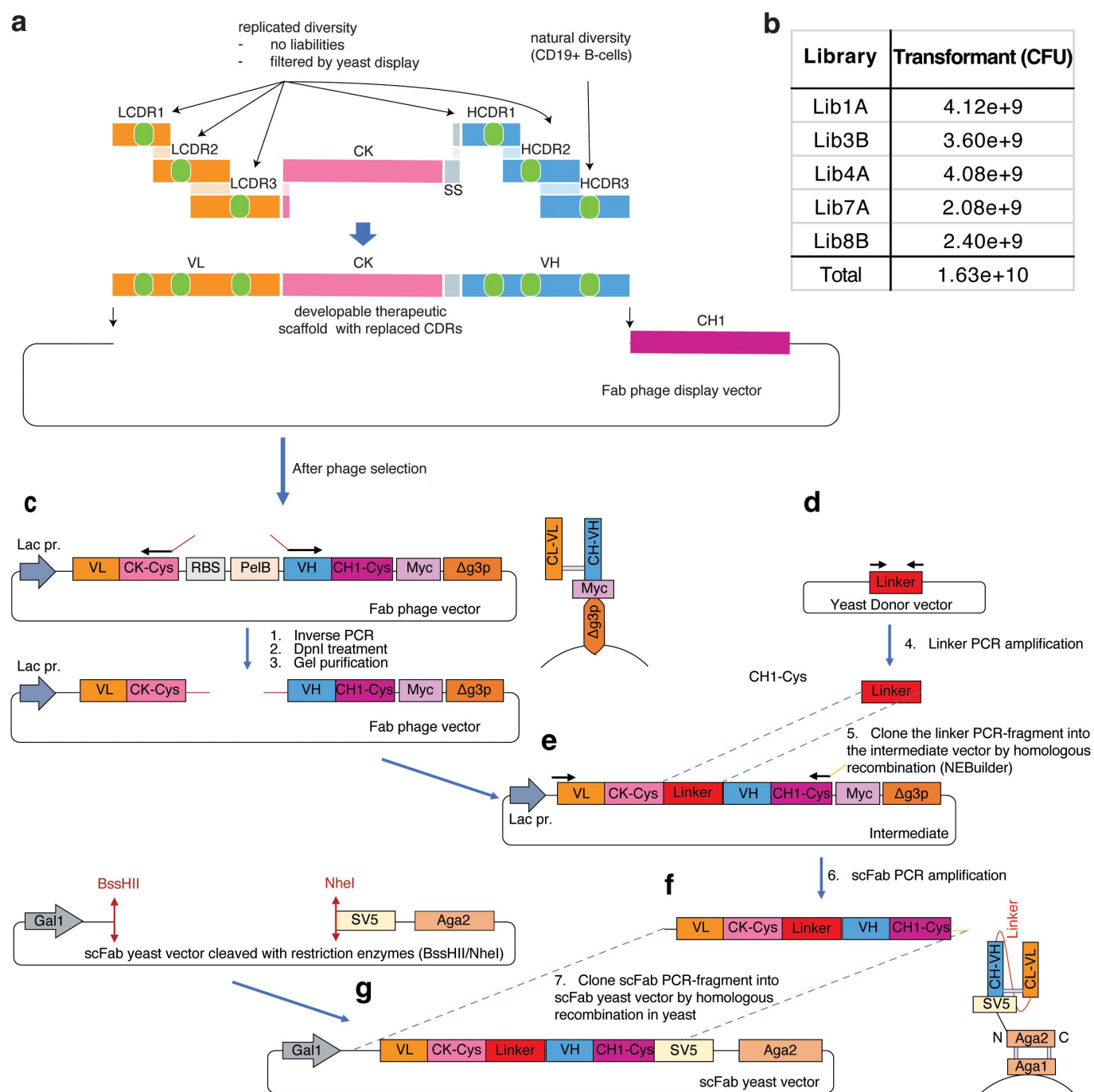


**Figure 2.** Schematic representation of the 2-step PCR conversion of Fab phage display into scFab yeast display. (a) graphic representation of the assembly strategy to generate the semi-synthetic Fab library. (b) number of transformants obtained after electroporation of each phage display sublibrary into *E. coli* TG1. (c) inverse-pcr based amplification of the phage display vector with a 5' primer annealing to the FW1 of the VH and 3' primer annealing to the end of the constant light chain region (CK), resulting in the linearization of the entire plasmid without the plasmid elements between the two domains constituting the Fab. (d) the primers confer complementary overhangs compatible to the 5' and 3' ends of a donor fragment amplified from the yeast DONOR vector. The donor fragment contains the linker for the generation of the scFab. (e) the intermediate vector is obtained by fusing the donor fragment in frame with the two domains of the Fab by NEBuilder® assembly kit. (f) the cassette from the intermediate vector pool is PCR amplified adding sequence homologous to the final yeast display vector at the ends of the fragment. (g) cloning of the cassette into the yeast display vector via homologous recombination.

“displayable” molecules were used for the final assembly. While it does not eliminate oligo synthesis and PCR errors, it does ensure that those retained do not compromise display.

HCDR3s were recovered from CD19+ cells from Leukopaks from 10 different human donors. After reverse transcription of the mRNA using an IgM-specific primer, the HCDR3s were amplified using a single universal reverse primer annealing to

the human JH region at the 3' end, and four different forward primers annealing to heavy framework 3 at the 5' end. The filtered CDRs obtained from the yeast mini-CDR libraries were assembled with the recovered HCDR3s by PCR, cloned into the phage display vector (Figure 2a) and transformed into *E. coli* TG1 cells, generating a total of  $\sim 1.6 \times 10^{10}$  transformants (Figure 2b).



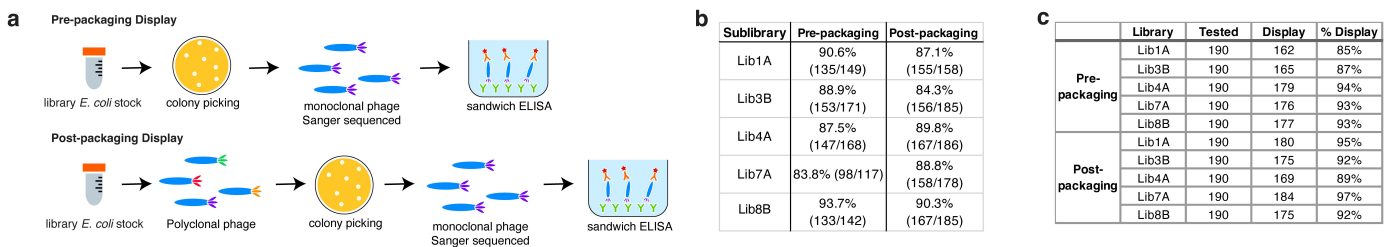


**Figure 3.** Quality control of the assembled library. a) schematic representation of the pre- and post-packaging experiments for evaluation of clone functionality and Sanger sequencing. Post-packaging refers to colonies picked after packaging the phagemid into phage particles and reinfecting cells, prepackaging refers to colonies picked directly from the library transformation. b) number of in-frame clones identified by Sanger sequencing in the naive library pre- and post-packaging. c) summary of Fab display levels of phage clones pre- and post-packaging tested by sandwich ELISA.

As quality control, the library was analyzed using: 1) Sanger sequencing for the assessment of open reading frames; 2) NGS by PacBio Sequel II for full-length analysis and clonal dominance, and Novaseq S4 for HCDR3 diversity analysis; and 3) enzyme linked immunosorbent assay (ELISA) for the assessment of Fab display on the phage surface. For the Sanger analysis, we sequenced clones immediately after transformation (prepackaging) and after producing the library as phage particles and reinfecting cells (post-packaging) (refer to Figure 3a for visual representation of pre- and post-packaging). We classified a clone as “functional” if it had a full-length in-frame sequence with no stop codons. No loss of functionality was observed in the packaging process, with an average functionality of 88.9% prepackaging (range 83.8%–93.7%) and 88.1% post-packaging (range 84.3%–90.3%) (Figure 3b).

We also produced monoclonal phage from colonies picked pre- and post-packaging, which allowed us to evaluate the display of Fab molecules at the bacteriophage surface. This assessment was done via a sandwich ELISA approach that included immobilization of an anti-Fab antibody in the microtiter plates to capture phage particles followed by incubation with an anti-M13 antibody (HRP conjugated). Again, no difference was observed between pre- and post-packaging, with a very high number of displaying clones in both cases (average of 90% (range from 85% to 94%) displaying clones prepackaging vs. 93% (range from 89% to 97%) displaying clones post-packaging (Figure 3c)).

These are interesting observations since nonfunctional clones, where the molecule is not expressed, are thought to have a growth advantage over clones containing open-reading frames and expressing antibodies. However, as the two domains of the Fab molecules (VL-CL, VH-CH1) are expressed by two cistrons, loss of functionality in one chain will not prevent the other from being expressed, perhaps limiting potential growth advantages.

Full-length Fab NGS using Pacbio Sequel II revealed no clonal dominance in the library, with the most frequently

**Table 2.** Frequency of the most dominant clone found in each library.

Library	Top 1 Clone frequency
Lib1A	0.00072%
Lib3B	0.00074%
Lib4A	0.00102%
Lib7A	0.00062%
Lib8B	0.00063%

observed clone representing only ~0.001% of the reads in Lib4A. However, the true frequency is likely less, as we are vastly under-sampling the diversity and this clone had only two reads (Table 2). We also verified the identity of the CDRs in the final library compared to the design and for the presence of liabilities. On average, 94.1% of the CDRs observed in the library matched designed sequences (range from 90.1% to 98.1%) (Table 3). Although non-matching CDRs are expected due to oligonucleotide synthesis and PCR-derived errors, they are always far less abundant than the designed CDRs (Supplementary Figures S2-S6). Since some sequences diverge from design, it is inevitable that sequence liabilities are inadvertently reintroduced. Nonetheless, more than 97% of the naturally replicated CDRs in clones analyzed in all libraries had no sequence liabilities (Figure 4a). Finally, the NovaSeq S4 platform was used to analyze the HCDR3 diversity of the final cloned library. A VH amplicon was produced by PCR and sequenced using NovaSeq S4 2 × 150bp. Reads were quality filtered, keeping only reads in which 90% of bases have a Q-score ≥30. Of  $5.3 \times 10^9$  reads,  $3.9 \times 10^9$  were retained for further analysis. HCDR3s were extracted using AbXtract ([www.eyesopen.com/orion/antibody-discovery-suite](http://www.eyesopen.com/orion/antibody-discovery-suite)), which identifies the 5' and 3' regions. HCDR3 sequences containing stop codons or frameshifts were excluded. The HCDR3 accumulation plot (Figure 4b) compares the HCDR3 diversities of Specifica's Generation 1<sup>15</sup> and Generation 2<sup>50</sup> scFv libraries with this Gen3 Fab library. The single sublibraries each contribute a similar number of unique HCDR3s (Figure 4c), and the final measured HCDR3 diversity is  $2.9 \times 10^8$ .

**Table 3.** Frequency of CDRs matching the designed sequences present in each library.

Region	Lib1A	Lib3B	Lib4A	Lib7A	Lib8B
LCDR1	97.97%	93.45%	96.95%	98.13%	98.01%
LCDR2	93.21%	90.09%	94.03%	93.67%	93.68%
LCDR3	95.59%	94.49%	94.02%	95.37%	96.04%
HCDR1	95.88%	95.17%	93.08%	95.47%	95.48%
HCDR2	93.86%	92.96%	95.82%	94.78%	95.66%

Finally, phages were produced from each of the sublibraries by superinfecting with the helper phage M13K07 for phage particle production, phage were titrated, and quality controlled by Western blot (Supplementary Figure S7).

### Fab phage library selection

To test the library performance, we carried out three rounds of phage display with human interferon- $\alpha$ -2b (hIFN $\alpha$ -2b) and SARS-CoV-2 receptor-binding domain (RBD). Titer enrichment was observed with the progression of selection rounds (Figure 5a), with more pronounced enrichment between rounds 2 and 3 of selection, as increased wash stringency was used between the 1st and 2nd rounds of selection and kept constant between the 2nd and 3rd rounds. From the final selection rounds (3rd), polyclonal phage populations were produced and tested in ELISA, where a strong specific polyclonal signal was detected for the specific target antigens. Fab display signal of the phage samples was also detected by coating an anti-Fab antibody on the ELISA plate (Figure 5b).

A phage ELISA screening was also conducted on randomly picked clones obtained after the 3rd round of selection for each target antigen. Ninety-five clones for each of the five sub-libraries and for each antigen were tested for their on- and off-target binding. The hit rate for each sub-library for hIFN $\alpha$ -2b ranged from 68% to 99%, while the hit rate for each sub-library for SARS-CoV-2 RBD ranged from 40% to 95%, as reported in Table 4 and Supplementary Figure S8.

The same clones screened by phage ELISA were Sanger sequenced. Only functional clones were reported. Unique clones were identified, using the same HCDR3 length and  $\geq 90\%$  identity in HCDR3 amino acid sequence to cluster variants. The number of unique clones for each campaign is reported in Tables 5–6. One cross-over clone (VL abrilumab and VH crenezumab) was identified as a binder against hIFN $\alpha$  2b. The unique HCDR3 sequence of binders is reported in Supplementary Table S3-S4. The HCDR3 were also aligned and those with at least 70% identity and matching the VL and VH scaffolds were grouped into the same cluster (Supplementary Tables S3-S4).

### From Fab phage display to scFab yeast display

The Fab-phage populations enriched after three rounds of selection for hIFN $\alpha$ -2b and SARS-CoV-2 RBD, were converted into scFab yeast display mini-libraries. This approach retains the original VH/VL pairing through a 2-step PCR strategy (Figure 2c–g). After subcloning and transforming the different libraires into the yeast display vector and yeast cells, the binding profiles were analyzed by flow cytometry at 0 nM (background for nonspecific binders to the secondary reagents) and 100 nM of the corresponding antigen (Figure 6a).

Overall, the yeast outputs had more than 48% display for both antigens. They all show some level of binding to their specific antigen, with libraries 3B, 4A and 8B more enriched for the SARS-CoV-2-RBD campaign, and libraries 1A, 4A and 8B more enriched for the hIFN $\alpha$ -2b campaign. However, the

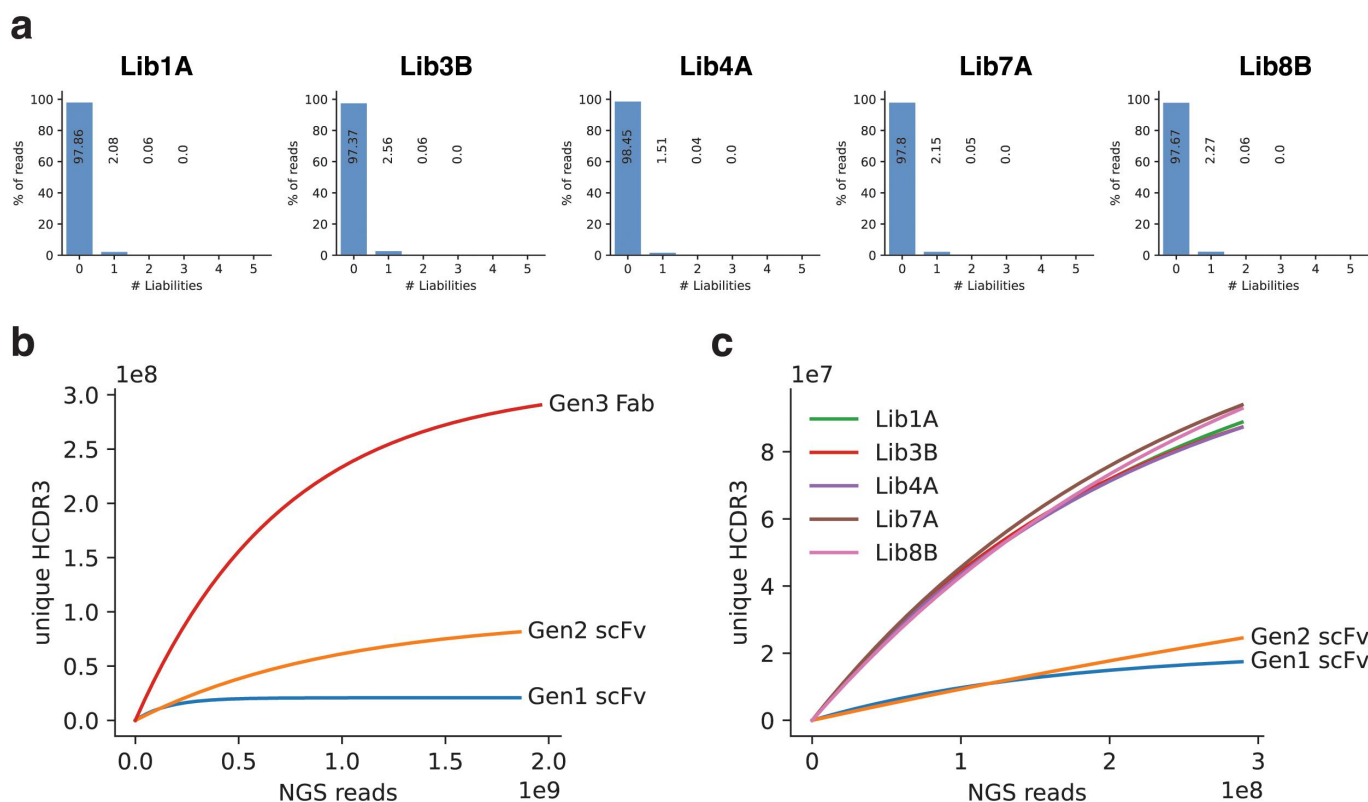


**Figure 4.** Quality control of the library by NGS. a) presence of sequence liabilities in the naturally replicated CDRs (HCDR1-2; LCDR1-3) used to generate sublibraries based on PacBio sequencing. b) accumulation plot of Fab library unique clones, compared to previous library iterations from NovaSeq sequencing analysis. c) accumulation plot of unique clones in the individual sublibraries.

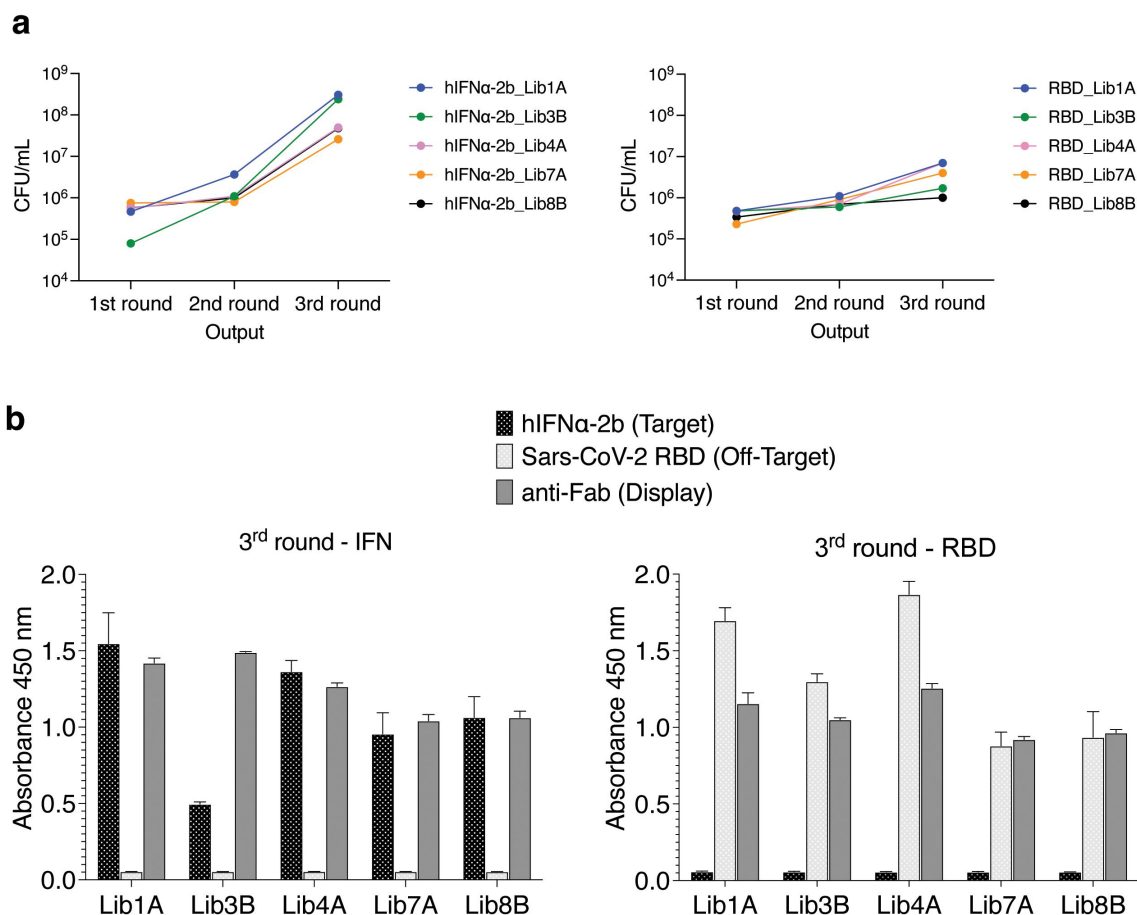


**Figure 5.** Antibody selection. a) enrichment of phage display selection titers for the 5 sub-libraries selected against hIFN $\alpha$ -2b and SARS-CoV-2 RBD. b) ELISA signals of polyclonal phage after 3 rounds of display tested against hIFN $\alpha$ -2b and SARS-CoV-2 RBD, which were also used as cross-reactivity controls for each over. Display levels were also tested (anti-Fab).

**Table 4.** Hit rates after the 3<sup>rd</sup> round of selection against hIFN $\alpha$ -2b and SARS-CoV-2 RBD as assessed by phage ELISA.

Library	Target antigen	#binders/#screened clones	% hits
Lib1A	hIFN $\alpha$ -2b	92/95	97%
Lib3B	hIFN $\alpha$ -2b	85/95	89%
Lib4A	hIFN $\alpha$ -2b	94/95	99%
Lib7A	hIFN $\alpha$ -2b	75/95	79%
Lib8B	hIFN $\alpha$ -2b	65/95	68%
Lib1A	SARS-CoV-2 RBD	88/95	93%
Lib3B	SARS-CoV-2 RBD	66/95	69%
Lib4A	SARS-CoV-2 RBD	90/95	95%
Lib7A	SARS-CoV-2 RBD	38/95	40%
Lib8B	SARS-CoV-2 RBD	73/95	77%

**Table 5.** Unique clones identified by Sanger sequencing of the 3<sup>rd</sup> round of selection on hIFN $\alpha$ -2b. Clones are classified regarding VL and VH scaffold and binding status.

VL Scaffold	VH Scaffold	Non-binders	Binders
Lib1A-VL-abrilumab	Lib1A-VH-abrilumab	3	47
Lib1A-VL-abrilumab	Lib3B-VH-crenezumab	0	1
Lib3B-VL-crenezumab	Lib3B-VH-crenezumab	6	30
Lib4A-VL-necitumumab	Lib4A-VH-necitumumab	1	21
Lib7A-VL-348	Lib7A-VH-348	15	32
Lib8B-VL-adalimumab	Lib8B-VH-adalimumab	22	12
	Total	47	143

levels of yeast positivity (4–45%) are somewhat lower than those observed in phage display, reflecting the possibility that PCR- or yeast-based recombination occurs either in the

constant portion of the amplified fragments (CK-linker) between the VH and VL genes during the transfer from phage to yeast, resulting in VH/VL shuffling, or within framework regions of either VH or VL genes, since these are preserved in each library.

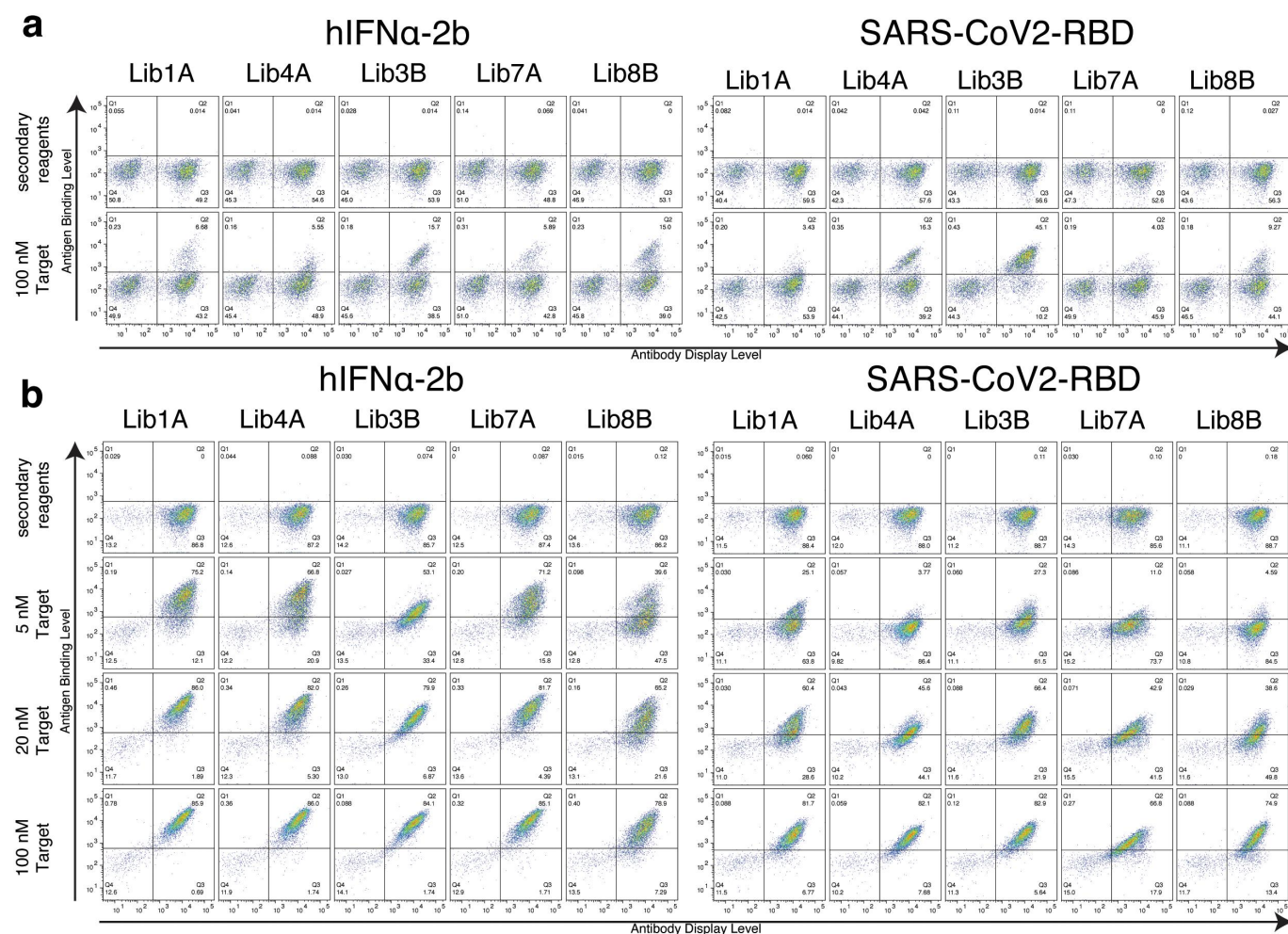
All five libraries were sorted for high-affinity binders for their respective antigens. The binding profile of the final populations were analyzed in the presence of different concentrations of antigen (Figure 6b). A sharp binding population was observed for all five libraries for both antigens, particularly at the higher concentrations, while a negligible binding population was observed in the absence of antigen. When decreasing the antigen concentration, the overall binding population decreased, but significant binding signals were present even at 5 nM.

### ScFab yeast library selection analysis

The scFab yeast display outputs were characterized in terms of diversity. For this purpose, 95 clones from the final output of each sublibrary and for each antigen were Sanger sequenced. As previously described for the Fab phage outputs, only functional clones were reported, and the unique clones were identified by HCDR3 diversity. As shown in Table 7, 69 and 24 unique HCDR3s were found from the hIFN $\alpha$ -2b and SARS-CoV-2-RBD campaigns, respectively, and all libraries

**Table 6.** Unique clones identified by Sanger sequencing of the 3<sup>rd</sup> round of selection on SARS-CoV-2 RBD. Clones are classified by VL and VH scaffold and binding status.

VL Scaffold	VH Scaffold	Non-binders	Binders
Lib1A-VL-abrilumab	Lib1A-VH-abrilumab	6	19
Lib3B-VL-crenezumab	Lib3B-VH-crenezumab	0	21
Lib4A-VL-necitumumab	Lib4A-VH-necitumumab	1	6
Lib7A-VL-348	Lib7A-VH-348	40	6
Lib8B-VL-adalimumab	Lib8B-VH-adalimumab	21	5
	Total	68	57

**Figure 6.** Sorting results of scFab yeast display. Flow cytometry analysis of scFab yeast display against hIFN $\alpha$ -2b and SARS-CoV-2 RBD, a) after directly subcloning the third rounds of phage display selection and b) after the final yeast sorting.

generated at least one antibody with a unique HCDR3 against each of the two antigens. These monoclonals were tested for target binding in yeast (Supplementary Figure S9 and S10), with clones considered positive if the binding value was at least five times greater than the signal obtained for the off-target antigen (Figure 7a–b). A total of 66 and 19 binders were found from the hIFN $\alpha$ -2b and SARS-CoV-2-RBD campaigns, respectively. The unique HCDR3 sequences of the binders are reported in Supplementary Tables S5–S6. The HCDR3 were also aligned and those with at least 70% identity and matching the VL and VH scaffolds were grouped into the same cluster (Supplementary Tables S5–S6).

Additionally, Fab and scFab sequences of binders isolated after phage and yeast selection, respectively, were

compared (Figure 7c). A total of 33 and 16 unique binding clones (same HCDR3) for the hIFN $\alpha$ -2b and SARS-CoV-2-RBD campaigns, respectively, were found in both the Fab and scFab formats, while 33 and 3 unique clones were only found as scFabs.

#### PacBio analysis of final Fab phage selection outputs and scFab yeast selection outputs

The final round populations from each selection campaign (phage and yeast display) for each of the sub-libraries were PCR amplified and sequenced using PacBio sequencing to capture the paired light and heavy chains. The expectation is

**Table 7.** Number of unique clones per sublibrary for each antigen identified after yeast sort of scFabs.

	hIFN $\alpha$ -2b		SARS-CoV-2-RBD	
	Unique HCDR3	Unique Binders on Yeast	Unique HCDR3	Unique Binders on Yeast
Lib1A	31	30	11	8
Lib3B	16	15	2	2
Lib4A	1	1	2	2
Lib7A	18	17	3	3
Lib8B	3	3	6	4
Total	69	66	24	19

that the phage outputs will be under-sampled by the PacBio platform (resulting in a focus on the most enriched clones), while the yeast outputs should be completely covered with 50,000 reads per sample (5 times the maximum expected diversity from the first yeast sort where 10,000 events were sorted). The number of functional reads per sample is shown in Supplementary Table S7. The reads were annotated using the IgMatcher tool, part of AbXtract ([www.eyesopen.com/orion/antibody-discovery-suite](http://www.eyesopen.com/orion/antibody-discovery-suite)), and scaffolds were assigned for VL and VH. Pairing for Fab and scFab outputs is reported in Figure 8a for the Fab phage outputs and Figure 8b for the scFab yeast outputs. Each sequenced clone was assigned to a library based on the scaffold pairing. Clones with mismatched VL and VH are reported as “other”. Clones with HCDR3s having the same length and  $\geq 90\%$  amino acid identity were merged. Sequences with abundance less than 0.005% were discarded. Following this analysis, 2942 and 6658 unique sequences were identified for the Fab phage campaigns against hIFN $\alpha$ -2b and SARS-CoV2-RBD, respectively (Figure 8c), and 436 and 106 unique sequences were identified for the scFab yeast campaigns against hIFN $\alpha$ -2b and SARS-CoV2-RBD, respectively (Figure 8d). As these sequences were only identified, binding activity cannot be ascertained without gene synthesis and further testing. Sequence liabilities were tabulated for all clones: for both selection campaigns using Fab phage (Supplementary Figure S11 for hIFN $\alpha$ -2b and Supplementary Figure S12 for SARS-CoV2-RBD),  $>95\%$  of naturally replicated CDRs had no sequence liabilities, and similar values were obtained after scFab yeast display where  $\geq 93\%$  of replicated CDRs had no sequence liabilities (Supplementary Figures S13 for hIFN $\alpha$ -2b and Supplementary Figures S14 for SARS-CoV2-RBD). The sequences of the Fab and scFab clones isolated at the end of the phage and yeast selection, respectively, were compared (Figure 8e,g for hIFN $\alpha$ -2b and Figure 8f,h for SARS-CoV2-RBD). A total of 388 and 66 unique clones (same HCDR3) were found in both the Fab and scFab formats, while 126 and 56 unique clones were only found as scFab, which could be explained by the under sampling of the Fab phage outputs by PacBio sequencing. The binding activity of the antibodies encoded by these sequences is unknown.

#### Assessment of conversion rate and binding activity of scFab into whole IgG molecules

All the scFab unique binding clones identified from the final yeast outputs against hIFN $\alpha$ -2b and SARS-CoV2-RBD (66 and

19, respectively) were converted into whole IgG molecules and expressed in Expi293F cells following the strategy described by Zhang et al.<sup>46</sup> Five days after transfection the concentration of recombinant IgG in cell culture supernatants were quantified by biolayer interferometry (Octet) using an anti-human IgG biosensor. The standard curves were generated using isotype matched IgG. The results of IgG expression levels in cell supernatants are shown in Figure 9a. More than 98% (84/85) of all the converted antibodies expressed at detectable levels of antibody, regardless of the target specificity, in the range of 0.05 to over 100  $\mu\text{g}/\text{mL}$ . The supernatants for each antigen were tested for binding specificity by ELISA. When tested on directly coated (non-biotinylated) antigen, 47/65 (72.3%) expressed IgGs against hIFN $\alpha$ -2b and 19/19 (100%) IgGs against SARS-CoV2-RBD demonstrated specific binding to their respective antigens (Figure 9b). When tested on indirectly coated antigen, with biotinylated antigen immobilized by interaction with neutravidin coated ELISA wells, the number of hIFN $\alpha$ -2b binders increased to 56/65 (86.2%) and remained at 100% binders (19/19) for SARS-CoV-2 RBD (Figure 9b). We speculate that the differences between the two hIFN $\alpha$ -2b data sets are due to the partial loss of some conformational epitopes when the antigen is directly coated on ELISA, and/or recognition of epitopes containing biotin used in the selection, reducing the binding efficiency of specific antibodies to the unmodified target.

#### Affinity and developability

The antibodies specifically recognizing the target in ELISA were expressed and purified in larger amounts to calculate their affinities and assess their developability proprieties. Affinities were measured by surface plasmon resonance (SPR) using the Catterra LSA-XT (plots shown in Supplementary Figures S15, S16 and S18). For the antibodies targeting hIFN $\alpha$ -2b, we observed 40/47 (85%) with clear binding profiles, of which (34/47) 72% exhibited non-complex binding profiles with a range of affinities from 18 pM to 74 nM, an interquartile range between 950 pM to 5.8 nM and a median affinity of 2.3 nM (Figure 10a and Supplementary Figures S17 and S19). 9/47 (19%) and 29/47 (62%) of the hIFN $\alpha$ -2b antibodies exhibited subnanomolar and single-digit nanomolar affinities, respectively, straight from selections. Many of the IFN-binding antibodies exhibited improved kinetic model fits upon reduction of the ligand density (Supplementary Figure S15 and 16). All the anti- SARS-CoV2-RBD antibodies were binders 19/19 (100%) with 15/19 (79%) exhibiting non-complex binding (Figure 10a and Supplementary Figure S18). Unlike the antibodies targeting

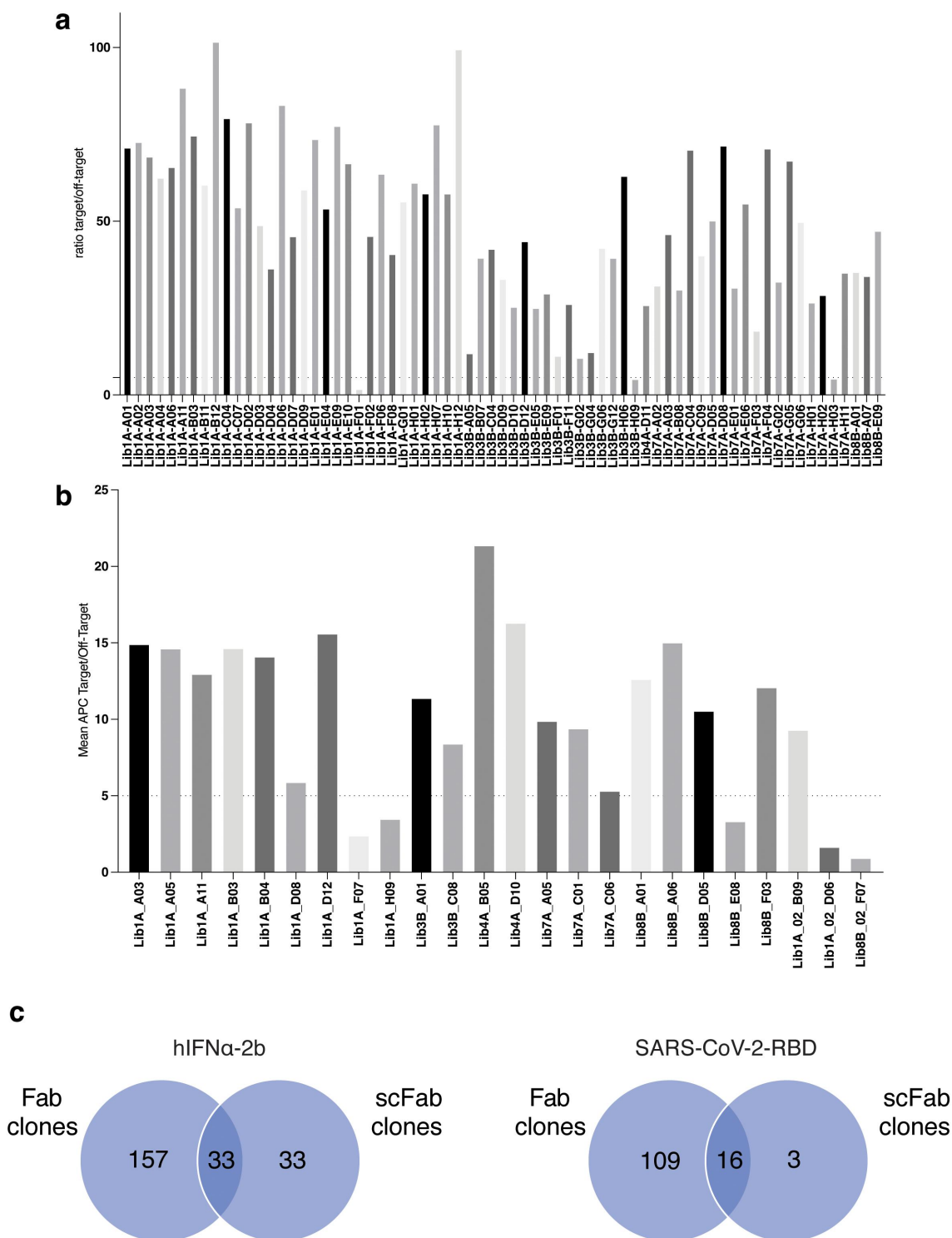


**Figure 7.** Fab phage scFab yeast outputs analysis. Binding activity of monoclonal scFab antibodies displayed on yeast against a) hIFN $\alpha$ -2b and b) SARS-CoV-2 RBD. Binding fold change over the off-target is reported. c) unique HCDR3s for each antigen isolated from the Fab-phage and the scFab-yeast selection outputs, with overlaps indicated.

hIFN $\alpha$ -2b, we were unable to improve any kinetic profiles of anti-RBD binding antibodies in repeated experiments. Of the 15 antibodies with non-complex binding profiles for 1:1 binding fit, we observed a range of affinities from 200 pM to 20 nM, an interquartile range between 1.4 nM and 7.0 nM and a median affinity of 4.1 nM. 3/19 (15%) and 14/19 (74%) of the anti-RBD antibodies exhibited subnanomolar affinities (Supplementary Figure S18 and S19).

All the antibodies recognizing the specific target at least in ELISA (47 against hIFN $\alpha$ -2b and 19 against SARS-CoV-2-RBD) were assessed for developability using different methods to provide insight into hydrophobicity, tendency for self-association, thermodynamic stability, aggregation propensity, colloidal stability, and electrostatics.

The hydrophobic properties were assessed by hydrophobic interaction chromatography (HIC) to gather insight

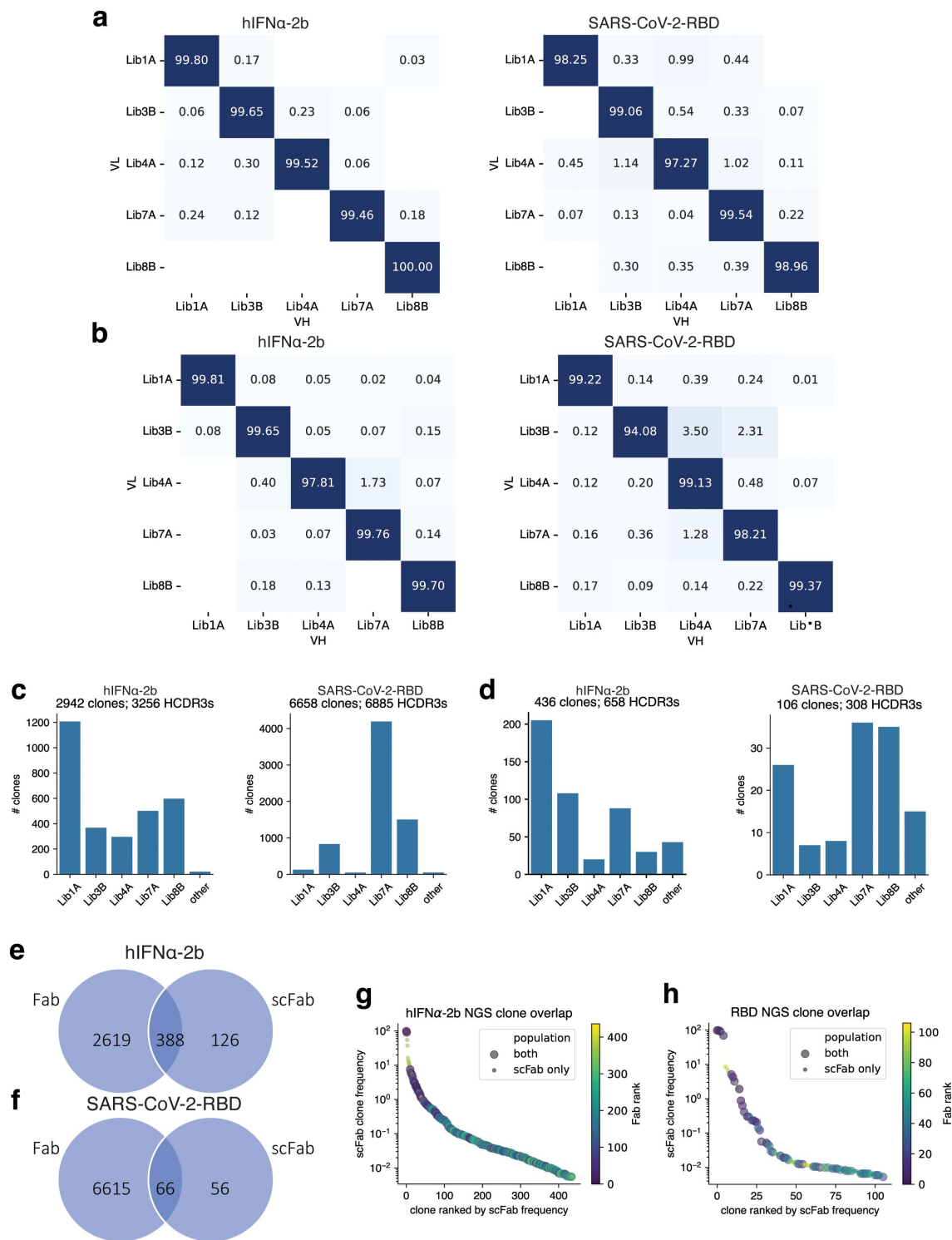


**Figure 8.** PacBio sequencing analysis of the selected scFab yeast clones. a) VL and VH scaffold pairing for both antigen Fab phage selection outputs. Values are normalized by VL (rows sum to 100%). b) VL and VH scaffold pairing for both antigen scFab yeast selection outputs. Values are normalized by VL (rows sum to 100%). c) number of unique clones identified from each sublibrary for each antigen for the Fab phage selection outputs. d) number of unique clones identified from each sublibrary for each antigen for the scFab yeast selection outputs. *The* number of unique HCDR3s for each antigen isolated from the Fab-phage and the scFab-yeast selection outputs identified by PacBio sequencing of the full Fab or scFab, and corresponding overlaps for e) hIFN $\alpha$ -2b and f) SARS-CoV-2 RBD. ScFab clones ranked by frequency for g) hIFN $\alpha$ -2b and h) SARS-CoV-2 RBD: large circles represent clones shared between scFab and Fab outputs and small circles represent clones exclusive to scFab output. Color indicates clones' respective rank in the Fab population with scFab-only clones taking on values greater than the highest ranked shared clone.

into relative percent purity of the main peak (Figure 10b). Most antibodies, 77% (49/66) exhibited favorable main peak purity (>70%) with a median value of 86.05% and interquartile range (IQR) from 71.58% to 93.85%. The

breakdown of the hydrophobicity of tested mAbs was target dependent: 85% (40/47) of the mAbs against hIFN $\alpha$ -2b exhibited more favorable properties, while only 53% (10/19) of antibodies against SARS-CoV2-RBD exhibited this

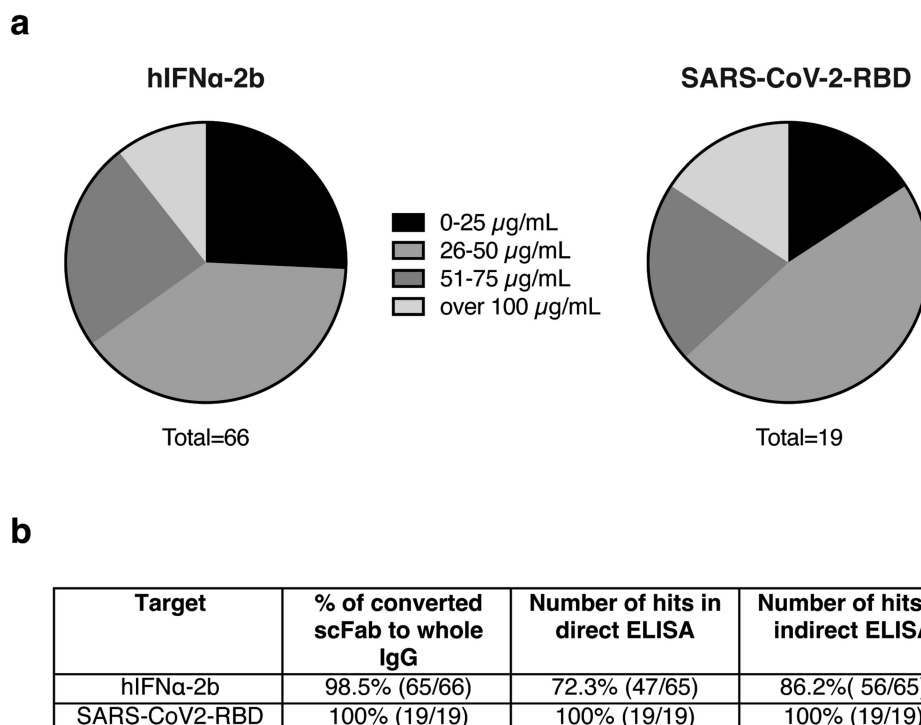


**Figure 9.** scFab to IgG conversion. a) IgG expression levels in supernatant of transfected Expi293F cells b) % IgG conversion and binding to corresponding target.

trend, indicating that antibody hydrophobic properties may be driven in part by antigen binding.

Size heterogeneity, related to potential aggregation and fractionation patterns of the antibodies, was determined by size-exclusion chromatography (SEC). A 95.4% (63/66) of antibodies exhibited favorable developability profiles with main peak purity values of  $\geq 80\%$  (Figure 10c). These antibodies exhibited median main peak values of 97.10% with an IQR of 95.7–97.8%.

Two metrics of melting temperature, ( $T_m$ ) and aggregation onset temperature ( $T_{\text{onset}}$ ), were used to understand antibody thermal stability profiles. A 100% (66/66) of the antibodies were above our preset threshold of 64°C, separating developable thermal profiles from non-developable (Figure 10d). The 64°C threshold is based on the upper threshold of the 10% worse 137 antibodies from Jain et al.<sup>48</sup> We observed 100% of the antibodies exhibiting a  $T_{\text{onset}}$  of above 50°C (Figure 10e), and all but one (98.5%) showed a  $T_{\text{onset}}$  of 55°C or higher.

Information pertaining to electrostatics (e.g., net charge) is an important criterion in antibody developability with high net charge typically correlated with poor developability. Capillary gel electrophoresis (cGE) was applied to gather insights into charge variants, in addition to aggregates and fragments that may also be present within the assay, by measuring variations in the % compared to the main peak. A large majority (91% – 60/66) of antibodies exhibited favorable values above 80% (Figure 10f), and the median % main peak purities were 85.25% with an IQR of 83.78–86.33%.

We investigated dynamic light scattering (DLS) at a UV absorbance of 280 nm to gain insight into the distribution of the antibodies in solutions, particularly as it pertains to size distribution, colloidal stability, monomericity and aggregation propensity. Acceptable ranges for peak interest of mean

diameter (nm), run from 5 to 20 nm, with 10–15 nm being optimal. Lower values suggest potential impurities, while higher values suggest the presence of larger molecular species (e.g., aggregates). A 93% of the clones exhibit a median value of 11.13 with an IQR of 10.85–11.71, indicating most antibodies are a homogenous population of monomeric antibodies (Figure 10g). The peak of interest mass (%) provides the relative mass of the main peak relative to other species. For these antibodies, we observed median values of 100% (mean = 96.6%) and an IQR of 100–100% (Figure 10h). This, coupled with the fact that 95% (63/66) of the antibodies exhibit favorable ( $\geq 95\%$ ) values, suggests a high level of purity and lower aggregation propensity.

Finally, the polydispersity index (PdI) provides insights into the relative size distribution for populations within the DLS measurement, with high values indicative of aggregates. The antibodies across all targets exhibit a median PdI of 0.06, with an IQR from 0.03 to 0.148 with 89% (59/66) (Figure 10i) exhibiting developable PdI values of  $< 0.2$  or values unable to be collected.

Upon examination of the cumulative failures for each antibody, we found that the bulk of the antibodies yielded either no or just one poor outcome out of all measurement parameters (Table 8). In particular, no red flags were observed for 60.6% (40/66) of antibodies, and 94% (62/66) of antibodies had one or zero red flags. A minor fraction of 4.5% (3/66) exhibited two red flags, whereas a single antibody, representing 1.5% of the total, displayed poor parameters in four of the described assays.

## Discussion

We previously reported<sup>6</sup> an *in vitro* scFv library platform able to generate antibodies with extremely high affinities,<sup>4,5,44</sup>



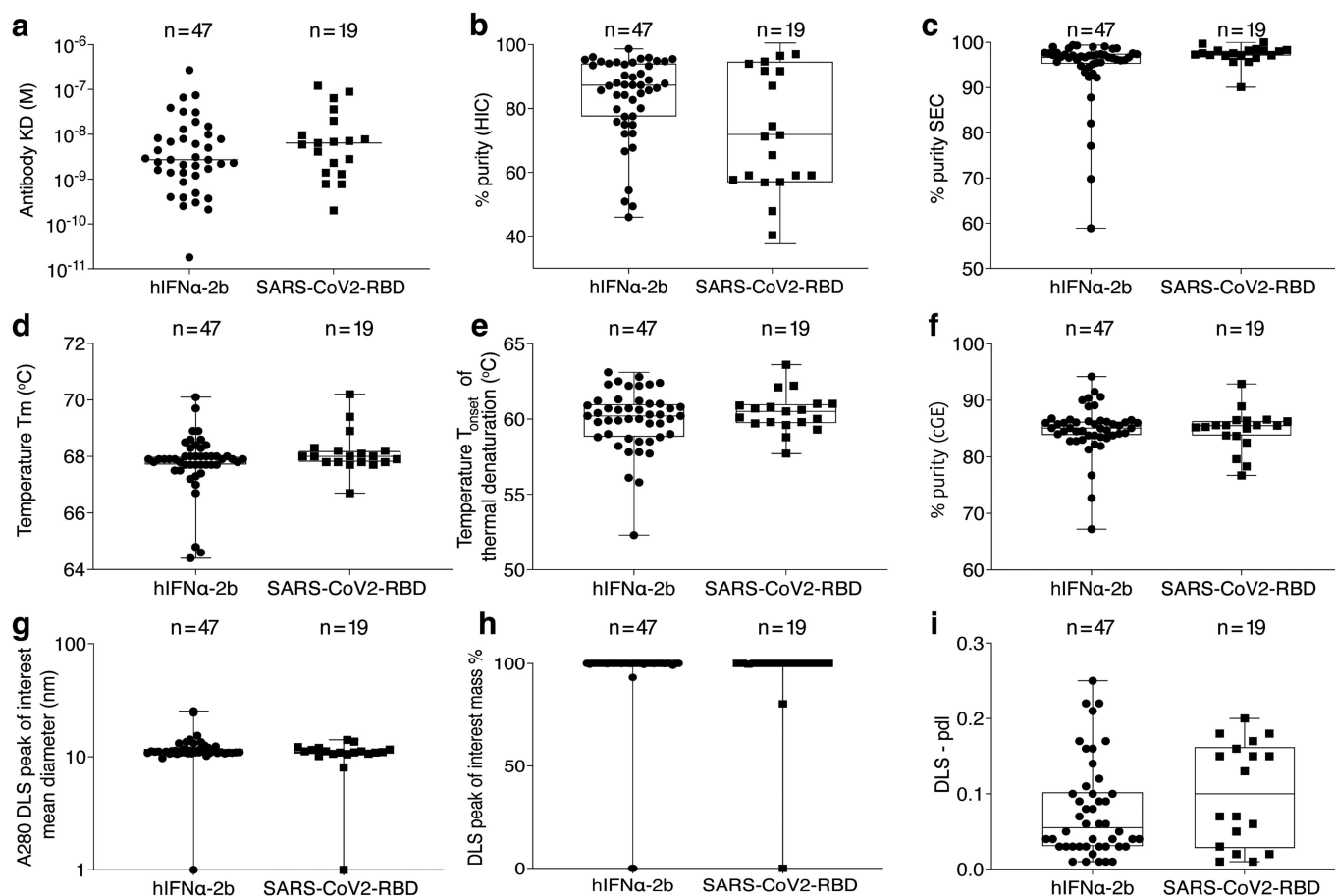


**Figure 10.** Developability assessment. All boxplots in each of the panels reflect the median, first quartile (25<sup>th</sup> percentile) and third quartile (75<sup>th</sup> percentile) of all the antibodies, with the whiskers reflecting 1.5× the interquartile range (IQR). All datapoints are plotted as jittered datapoints across the plot using the varying metrics with dark blue values indicative of acceptable developable readings and dark red indicating poorly developable measurements. a) antibody affinities measured by surface plasmon resonance (SPR). b) aggregation and fractionation by size-exclusion chromatography (SEC) expressed as a percentage of the main peak using the area under the curve (AUC). c) hydrophobicity profiles assessed by hydrophobic interaction chromatography (HIC), with the AUC of the main peak expressed relative to other peaks across the profile. Fab stabilities determined by d) melting temperature ( $T_m$ ) collected using the BCM of the fluorescence data from the inflection point (maximum of the first derivative) of the thermal profile and e) the aggregation onset temperature ( $T_{onset}$ ) in which we observe a significant elevation of the SLS data. Charge variants were assessed by f) capillary gel electrophoresis (cGE) assessing the AUC of the main peak relative to other peaks across the profile. Aggregate or impurities were analyzed by dynamic light scattering (DLS) at 280 nm absorbance to measure g) the peak of interest mean diameter (nm), h) the peak of interest mass percent (%) and i) the Polydispersity Index (Pdl), a unitless metric.

**Table 8.** Number of cumulative developability “red flags” in individual assay by antibody.

# Red flags	Total	%
0	40	60.6
1	22	33.3
2	3	4.5
3	0	0.0
4	1	1.5

which in many cases were better than those derived from immune sources and exhibited correspondingly more potent biological activity.<sup>5</sup> The success of this platform was based on several design factors: 1) The use of highly developable clinical antibodies as scaffolds; 2) Naturally replicated CDR diversity, derived from NGS of B cell variable genes and matched to scaffold germline genes for all CDRs but HCDR3; 3) Elimination of all sequence liabilities from naturally replicated CDRs; 4) HCDR3 diversity derived from donor B cells by PCR and quantified by NGS; and 5) The combination of phage and

yeast display to select antibodies. Here, we extend these findings to a novel variation of the platform that uses Fab in phage display and scFab in yeast display.

The scFab format<sup>36–43</sup> is a relatively novel and less widely used format for antibody display and selection, in which VH-CH1 and VL-CL are connected by a flexible linker. This is expected to have a number of advantages over the Fab and scFv formats, including: 1) scFabs have been successfully displayed on yeast; 2) scFab display requires only one signal peptide for export to the yeast surface, instead of the two for conventional Fab molecules; 3) light and heavy chains are expressed at identical levels with no need to balance their expressions; 4) combining the light and heavy chains in a single polypeptide ensures more efficient pairing of the two chains, avoiding the need for VH-CH1 and VL-CL to associate, and the possibility of unpaired VH-CH1 chains conferring specific binding activity;<sup>27,33,34</sup> 5) conversion from scFab to IgG is likely to be more efficient than from scFv; and 6) the single-gene construct is more

straightforward to manipulate genetically than the two gene Fab format or the use of yeast mating and two independent vectors<sup>27</sup> to create Fab libraries.

The Fab phage library was designed and engineered using the same strategy previously described for a highly effective scFv phage/yeast platform.<sup>4,6,44</sup> Four well-behaved therapeutic antibodies (and an additional non-therapeutic scaffold), all of which could be functionally displayed on phage, were chosen as scaffolds. These overlapped with, but differed from, those scaffolds used for scFv. Sequences encoding natural, germline-matched CDR diversity for all CDRs, except HCDR3, were purged of sequence liabilities *in silico*, synthesized on arrays, cloned into single CDR scFv libraries, and filtered by bulk selection using yeast display to eliminate sequences encoding poorly displaying CDRs. This process eliminated CDRs that did not fold within the desired scaffold, as well as any potential issues stemming from oligonucleotide synthesis or PCR errors that may affect display. As HCDR3 diversity exceeds oligo synthesis capacity and is far greater than that of the other CDRs, it was sourced by amplification from 10 healthy donors, using NovaSeq NGS to determine a final diversity of  $\sim 2.9 \times 10^8$  unique HCDR3 sequences. Library quality was further assessed using PacBio to sequence a PCR product encompassing the entire Fab molecule. As expected, this confirmed the rarity of sequence-based liabilities in all CDRs except HCDR3, as well as the absence of clonal dominance. Within the context of the complete library, the abundance of the most prevalent clone/s in each sublibrary was calculated at  $\sim 0.0002\%$ , representing an extremely flat distribution. To assess clonal genotypic stability and library display, Sanger sequencing and Western blotting were carried out before and after packaging into phage particles. This revealed there was no increase in nonfunctional clones or reduced display levels after phage packaging, attesting to the library's successful construction and functionality.

Antibodies were selected against two targets, IFN and the RBD of the SARS-CoV-2 spike protein. Phage antibodies were tested for binding after three rounds of phage selection, after which phage outputs were cloned into the scFab yeast display format using a two-step PCR approach. Only a limited number of clones identified during phage ELISA screening after phage selection was also found in the final scFab populations after yeast sorting. We speculate this reflects enrichment (with consequent diversity reduction) of higher affinity antibodies during yeast display, compared to those selected only by phage display, although it is also possible that certain clones may display or bind to antigens better when displayed as Fab on phage, rather than as scFab on yeast. Our hypothesis is that when clones are screened in phage ELISA as monoclonals, the signal is usually qualitative rather than quantitative. The nature of an ELISA assay allows the identification of binders with low affinity (up to  $\mu\text{M}$  binders). Moreover, due to the high-throughput nature of the assay, each individual clone cannot be titrated (i.e., using the same number of phage per clone), and the display of molecules on the surface of filamentous phage varies from 1 to  $\sim 30\%$ . Consequently, clones with relatively poor affinity can still be identified as binders in the phage format, but when these phage outputs are converted into yeast, the populations lose poor affinity binders during yeast sorting, as

well as those clones that may have a growth advantage in *E. coli* compared to *S. cerevisiae*. As a result, poorly behaving antibodies are filtered out.

We expected conversion of scFab to Fab or IgG to be more efficient than conversion from the scFv format (which in our hands ranges from 74% to 92%, depending upon target and scaffold, but with an 86% overall conversion rate<sup>7</sup>), although there are published examples to the contrary.<sup>43</sup> With 95 clones screened for each target, a diverse panel of binding scFabs was isolated (47 and 19 for IFN and RBD, respectively). An 86% of hIFN $\alpha$ -2b scFabs, 100% of SARS-CoV2-RBD scFabs (and 89% overall) were successfully converted to functional IgGs if binding against unmodified and biotinylated targets are taken together, representing a slight improvement over scFv conversion to IgG. We plan to expand the conversion rate assessment to include a larger number of antibodies targeting various antigens in order to understand whether this slight improvement is statistically significant. Converted IgGs were found to have high affinities directly from the library (18 pM best affinity) and excellent developability properties (Figure 10), with a majority of antibodies having no developability red flags. Consequently, most antibodies were already drug-like in their properties, and potentially without the need for further improvement.

The results of the present study show the value of the scFab format in the selection of specific and developable antibodies, such that the construction of a novel scFab phage antibody library could further streamline the process of transitioning from phage to yeast (Supplementary Figure S20).

This study showcases the compatibility of a well-established pipeline for selecting recombinant antibodies using phage and yeast display<sup>2,3</sup> to select functional antibodies from a highly efficient semi-synthetic library design.<sup>6</sup> Specifically, the use of Fab and scFab was utilized as displayed antibody molecules, for phage and yeast display, respectively, a strategic approach that effectively enabled the identification of specific antibodies with favorable developability profiles and good conversion into full-length IgG.

## Acknowledgments

We acknowledge Drew Wiesel, Nazzareno Dimasi, Nicolas Mouz, Emmanuelle Vigne and Carla D'Avanzo from Sanofi for their experimental feedback and support during the project.

This work was financially supported by Sanofi.

## Disclosure statement

FF, AF, EM, AD, SD, MFA, LS, JL, TJP and ARMB are employees of Specifica, a Q<sup>2</sup> lab solutions company. CLL, KD, CM and SK are employees of Sanofi and may hold stock or stock options.

## Funding

The author(s) reported that there is no funding associated with the work featured in this article.

## ORCID

Fortunato Ferrara  <http://orcid.org/0000-0002-4615-035X>

Adeline Fanni  <http://orcid.org/0000-0002-7240-2792>  
 Andre A. R. Teixeira  <http://orcid.org/0000-0002-8348-0235>  
 Esteban Molina  <http://orcid.org/0000-0039-2813-5997>  
 Camila Leal-Lopes  <http://orcid.org/0000-0001-7058-3350>  
 Ashley DeAgüero  <http://orcid.org/0000-0001-7110-9167>  
 Sara D'Angelo  <http://orcid.org/0000-0002-8329-9938>  
 M. Frank Erasmus  <http://orcid.org/0000-0002-8046-5048>  
 Laura Spector  <http://orcid.org/0000-0002-3965-9115>  
 Luis Antonio Rodríguez Carnero  <http://orcid.org/0000-0003-0684-4039>  
 Jianquan Li  <http://orcid.org/0009-0004-3205-9514>  
 Thomas J. Pohl  <http://orcid.org/0000-0002-8182-3249>  
 Nikolai Suslov  <http://orcid.org/0009-0009-3229-1854>  
 Conor McMahon  <http://orcid.org/0000-0001-9971-7869>  
 Sagar Kathuria  <http://orcid.org/0000-0003-3670-4467>  
 Andrew R. M. Bradbury  <http://orcid.org/0000-0002-5567-8172>

## Author's contributions

Originators of project: KD, NS, FF, SD, AART, ARMB.  
 Participated in research design: KD, NS, FF, SD, AART, ARMB.  
 Conducted experiments: FF, AF, AART, EM, CL, AD, MFE, LARC, JL, TP, SK.  
 Performed data analysis: FF, AF, MFE, LS, SK.  
 Wrote or contributed to the writing of the manuscript: FF, AF, AART, EM, CL, AD, SD, MFE, LS, LARC, JL, TP, KD, NS, SK, CM and ARMB.

## Abbreviations

scFv single-chain variable fragment.  
 Fab antigen-binding fragment.  
 scFab single-chain antigen-binding fragment.  
 CDR complementary-determining region.  
 VH heavy chain variable domain.  
 VL light chain variable domain.  
 IgG immunoglobulin G.

## References

- Bradbury AR, Sidhu S, Dübel S, McCafferty J. Beyond natural antibodies: the power of in vitro display technologies. *Nat Biotechnol.* 2011;29(3):245–254.
- Ferrara F, Naranjo LA, Kumar S, Gaiotto T, Mukundan H, Swanson B, Bradbury AR. Using phage and yeast display to select hundreds of monoclonal antibodies: application to antigen 85, a tuberculosis biomarker. *PLOS ONE.* 2012;7(11):e49535.
- Ferrara F, D'Angelo S, Gaiotto T, Naranjo L, Tian H, Gräslund S, Dobrovetsky E, Hraber P, Lund-Johansen F, Saragoza S, et al. Recombinant renewable polyclonal antibodies. *MABs.* 2015;7(1):32–41. doi:10.4161/19420862.2015.989047.
- Ferrara F, Erasmus MF, D'Angelo S, Leal-Lopes C, Teixeira AA, Choudhary A, Honnen W, Calianese D, Huang D, Peng L, et al. A pandemic-enabled comparison of discovery platforms demonstrates a naive antibody library can match the best immune-sourced antibodies. *Nat Commun.* 2022;13(1):462.
- Erasmus MF, Ferrara F, D'Angelo S, Spector L, Leal-Lopes C, Teixeira AA, Sørensen J, Nagpal S, Perea-Schmitt K, Choudhary A, et al. Insights into next generation sequencing guided antibody selection strategies. *Sci Rep.* 2023;13(1):18370. doi:10.1038/s41598-023-45538-w.
- Teixeira AAR, Erasmus MF, D'Angelo S, Naranjo L, Ferrara F, Leal-Lopes C, Durrant O, Galmiche C, Morelli A, Scott-Tucker A, et al. Drug-like antibodies with high affinity, diversity and developability directly from next-generation antibody libraries. *MABs.* 2021;13(1):1980942. doi:10.1080/19420862.2021.1980942.
- Franca RKA, Studart IC, Bezerra MR, Pontes LQ, Barbosa AM, Brigido MM, Furtado, GP, Maranhão AQ. Progress on phage display technology: tailoring antibodies for cancer immunotherapy. *Viruses.* 2023;15(9):1903.
- Wang Z, Wang G, Lu H, Li H, Tang M, Tong A. Development of therapeutic antibodies for the treatment of diseases. *Mol Biomed.* 2022;3(1):35.
- Zhang Y. Evolution of phage display libraries for therapeutic antibody discovery. *MABs.* 2023;15(1):2213793. doi:10.1080/19420862.2023.2213793.
- Huston JS, Levinson D, Mudgett-Hunter M, Tai, MS, Novotný J, Margolies MN, Ridge RJ, Brucoleri RE, Haber E, Crea R. Protein engineering of antibody binding sites: recovery of specific activity in an anti-digoxin single-chain Fv analogue produced in *Escherichia coli*. *Proc Natl Acad Sci USA.* 1988;85(16):5879–5883.
- Marks JD, Hoogenboom HR, Bonnert TP, McCafferty J, Griffiths AD, Winter G. By-passing immunization. Human antibodies from V-gene libraries displayed on phage. *J Mol Biol.* 1991;222(3):581–597.
- Barbas CF 3rd, Bain JD, Hoekstra DM, Lerner RA. Semisynthetic combinatorial antibody libraries: a chemical solution to the diversity problem. *Proc Natl Acad Sci USA.* 1992;89(10):4457–4461.
- Vaughan TJ, Williams AJ, Pritchard K, Osbourn JK, Pope AR, Earnshaw JC, McCafferty J, Hodits RA, Wilton J, Johnson KS, et al. Human antibodies with sub-nanomolar affinities isolated from a large non-immunized phage display library. *Nat Biotechnol.* 1996;14(3):309–14. doi:10.1038/nbt0396-309.
- Pini A, Viti F, Santucci A, Carnemolla B, Zardi L, Neri P, Neri D. Design and use of a phage display library. Human antibodies with subnanomolar affinity against a marker of angiogenesis eluted from a two-dimensional gel. *J Biol Chem.* 1998;273(34):21769–76.
- Sblattero D, Bradbury A. Exploiting recombination in single bacteria to make large phage antibody libraries. *Nat Biotechnol.* 2000;18(1):75–80. doi:10.1038/71958.
- Soderlind E, Strandberg L, Jirholt P, Kobayashi N, Alexeiva V, Åberg AM, Nilsson A, Jansson B, Ohlin M, Wingren C, et al. Recombining germline-derived CDR sequences for creating diverse single-framework antibody libraries. *Nat Biotechnol.* 2000;18(8):852–856.
- Griffiths AD, Williams SC, Hartley O, Tomlinson, IM, Waterhouse P, Crosby WL, Kontermann RE, Jones, PT, Low NM, Allison TA. Isolation of high affinity human antibodies directly from large synthetic repertoires. *Embo J.* 1994;13(14):3245–3260.
- Hoet RM, Cohen EH, Kent RB, Rookey K, Schoonbroodt S, Hogan S, Rem L, Frans N, Daukandt M, Pieters H, et al. Generation of high-affinity human antibodies by combining donor-derived and synthetic complementarity-determining-region diversity. *Nat Biotechnol.* 2005;23(3):344–348. doi:10.1038/nbt1067.
- Zhu Z, Dimitrov DS. Construction of a large naive human phage-displayed fab library through one-step cloning. *Methods Mol Biol.* 2009;525:129–142, xv.
- Solfrosi L, Mancini N, Canducci F, Clementi N, Sautto GA, Diotti RA, Clementi M, Burioni R. A phage display vector optimized for the generation of human antibody combinatorial libraries and the molecular cloning of monoclonal antibody fragments. *New Microbiologica.* 2012;35(3):289–294.
- Tiller T, Schuster I, Deppe D, Siegers K, Strohnner R, Herrmann T, Berenguer M, Poujol D, Stehle J, Stark Y, et al. A fully synthetic human Fab antibody library based on fixed VH/VL framework pairings with favorable biophysical properties. *MABs.* 2013;5(3):445–470. doi:10.4161/mabs.24218.
- Kugler J, Wilke S, Meier D, Tomszak F, Frenzel A, Schirrmann T, Dübel S, Garritsen H, Hock B, Toleikis L, et al. Generation and analysis of the improved human HAL9/10 antibody phage display libraries. *BMC Biotechnol.* 2015;15(1):10. doi:10.1186/s12896-015-0125-0.
- Kim S, Park I, Park SG, Cho S, Kim JH, Ipper NS, Choi SS, Lee ES, Hong HJ. Generation, diversity determination, and application to antibody selection of a human naive fab library. *Mol Cells.* 2017;40(9):655–666.

24. Maruthachalam BV, El-Sayed A, Liu J, Sutherland AR, Hill W, Alam MK, Pastushok L, Fonge H, Barreto K, Geyer CR, et al. A single-framework synthetic antibody library containing a combination of canonical and variable complementarity-determining regions. *Chembiochem*. 2017;18(22):2247–2259. doi:10.1002/cbic.201700279.
25. Rippmann JF, Klein M, Hoischen C, Brocks B, Rettig WJ, Gumpert J, Pfizenmaier K, Mattes R, Moosmayer D. Prokaryotic expression of single-chain variable-fragment (scFv) antibodies: secretion in L-form cells of *Proteus mirabilis* leads to active product and overcomes the limitations of periplasmic expression in *Escherichia coli*. *Appl Environ Microbiol*. 1998;64(12):4862–4869.
26. Marks JD, Hoogenboom HR, Griffiths AD, Winter G. Molecular evolution of proteins on filamentous phage. Mimicking the strategy of the immune system. *J Biol Chem*. 1992;267(23):16007–16010.
27. Weaver-Feldhaus JM, Lou J, Coleman JR, Siegel RW, Marks JD, Feldhaus MJ. Yeast mating for combinatorial Fab library generation and surface display. *FEBS Lett*. 2004;564(1–2):24–34.
28. Labrijn AF, Poignard P, Raja A, Zwick MB, Delgado K, Franti M, Binley J, Vivona V, Grundner C, Huang C-C, et al. Access of antibody molecules to the conserved coreceptor binding site on glycoprotein gp120 is sterically restricted on primary human immunodeficiency virus type 1. *J Virol*. 2003;77(19):10557–10565. doi:10.1128/JVI.77.19.10557-10565.2003.
29. Skerra A, Pfitzinger I, Pluckthun A. The functional expression of antibody Fv fragments in *Escherichia coli*: improved vectors and a generally applicable purification technique. *Biotechnol (N Y)*. 1991;9(3):273–278.
30. Feldhaus MJ, Siegel RW, Opreko LK, Coleman JR, Feldhaus JM, Yeung YA, Cochran JR, Heinzelman P, Colby D, Swers J, et al. Flow-cytometric isolation of human antibodies from a nonimmune *Saccharomyces cerevisiae* surface display library. *Nat Biotechnol*. 2003;21(2):163–170. doi:10.1038/nbt785.
31. van den Beucken T, Pieters H, Steukers M, van der Vaart M, Ladner RC, Hoogenboom HR, Hufton SE. Affinity maturation of Fab antibody fragments by fluorescent-activated cell sorting of yeast-displayed libraries. *FEBS Lett*. 2003;546(2–3):288–294.
32. Blaise L, Wehnert A, Steukers MP, van den Beucken T, Hoogenboom HR, Hufton SE. Construction and diversification of yeast cell surface displayed libraries by yeast mating: application to the affinity maturation of Fab antibody fragments. *Gene*. 2004;342(2):211–218.
33. Gargano N, Biocca S, Bradbury A, Cattaneo A. Human recombinant antibody fragments neutralizing human immunodeficiency virus type 1 reverse transcriptase provide an experimental basis for the structural classification of the DNA polymerase family. *J Virol*. 1996;70(11):7706–7712.
34. Gargano N, Cattaneo A. Inhibition of murine leukaemia virus retrotranscription by the intracellular expression of a phage-derived anti-reverse transcriptase antibody fragment. *J Gen Virol*. 1997;78(Pt 10):2591–2599.
35. Lee HS, Shu L, De Pascalis R, Giuliano M, Zhu M, Padlan EA, Hand PH, Schlom J, Hong HJ, Kashmiri SV. Generation and characterization of a novel single-gene-encoded single-chain immunoglobulin molecule with antigen binding activity and effector functions. *Mol Immunol*. 1999;36(1):61–71.
36. Hust M, Jostock T, Menzel C, Voedisch B, Mohr A, Brenneis M, Kirsch MI, Meier D, Dübel S. Single chain Fab (scFab) fragment. *BMC Biotechnol*. 2007;7:14.
37. Jordan E, Al-Halabi L, Schirrmann T, Hust M, Dübel S. Production of single chain Fab (scFab) fragments in *Bacillus megaterium*. *Microb Cell Fact*. 2007;6(1):38. doi:10.1186/1475-2859-6-38.
38. Koerber JT, Hornsby MJ, Wells JA. An improved single-chain Fab platform for efficient display and recombinant expression. *J Mol Biol*. 2015;427(2):576–586.
39. Walker LM, Bowley DR, Burton DR. Efficient recovery of high-affinity antibodies from a single-chain Fab yeast display library. *J Mol Biol*. 2009;389(2):365–375.
40. Sivelse C, Sierocki R, Ferreira-Pinto K, Simon S, Maillere B, Nozach H. Fab is the most efficient format to express functional antibodies by yeast surface display. *MAbs*. 2018;10(5):1–34. doi:10.1080/19420862.2018.1468952.
41. Hanna R, Cardarelli L, Patel N, Blazer LL, Adams JJ, Sidhu SS. A phage-displayed single-chain Fab library optimized for rapid production of single-chain IgGs. *Protein Sci*. 2020;29(10):2075–2084.
42. Chang J, Rader C, Peng H. A mammalian cell display platform based on scFab transposition. *Antib Ther*. 2023;6(3):157–169.
43. Steinwand M, Droste P, Frenzel A, Hust M, Dübel S, Schirrmann T. The influence of antibody fragment format on phage display based affinity maturation of IgG. *MAbs*. 2014;6(1):204–218. doi:10.4161/mabs.27227.
44. Erasmus MF, Dovner M, Ferrara F, D'Angelo S, Teixeira AA, Leal-Lopes C, Spector L, Hopkins E, Bradbury ARM. Determining the affinities of high-affinity antibodies using KinExA and surface plasmon resonance. *MAbs*. 2023;15(1):2291209. doi:10.1080/19420862.2023.2291209.
45. Boder ET, Wittrup KD. Yeast surface display for screening combinatorial polypeptide libraries. *Nat Biotechnol*. 1997;15(6):553–557. doi:10.1038/nbt0697-553.
46. Zhang R, Prabakaran P, Yu X, Mackness BC, Boudanova E, Hopke J, Sancho J, Saleh J, Cho H, Zhang N, et al. A platform-agnostic, function first-based antibody discovery strategy using plasmid-free mammalian expression of antibodies. *MAbs*. 2021;13(1):1904546. doi:10.1080/19420862.2021.1904546.
47. Estep P, Caffry I, Yu Y, Sun T, Cao Y, Lynaugh H, Jain T, Vásquez M, Tessier PM, Xu Y. An alternative assay to hydrophobic interaction chromatography for high-throughput characterization of monoclonal antibodies. *MAbs*. 2015;7(3):553–561. doi:10.1080/19420862.2015.1016694.
48. Jain T, Sun T, Durand S, Hall A, Houston NR, Nett JH, Sharkey B, Bobrowicz B, Caffry I, Yu Y, et al. Biophysical properties of the clinical-stage antibody landscape. *Proc Natl Acad Sci USA*. 2017;114(5):944–949. doi:10.1073/pnas.1616408114.
49. Teixeira AAR, Erasmus MF, D'Angelo S, Naranjo L, Ferrara F, Leal-Lopes C, Durrant O, Galmiche C, Morelli A, Scott-Tucker A, et al. Drug-like antibodies with high affinity, diversity and developability directly from next-generation antibody libraries. *MAbs*. 2021.13(1). Taylor & Francis. doi:10.1080/19420862.2021.1980942.
50. Erasmus MF, D'Angelo S, Ferrara F, Naranjo L, Teixeira AA, Buonpane R, Stewart SM, Natri HG, Bradbury AR. A single donor is sufficient to produce a highly functional in vitro antibody library. *Commun Biol*. 2021;4(1):350.